Two distinct Precambrian terranes in the Southern Prince Charles Mountains, East Antarctica: SHRIMP dating and geochemical constraints

E.V. Mikhalsky [a,*], B.V. Beliatsky [b], J.W. Sheraton [c], N.W. Roland [d]

[a] VNIIOkeangeologia, Angliisky str., 1, 190121 St Petersburg, Russia
[b] IGGP, Makarova emb., 2, 199034 St Petersburg, Russia
[c] Stoneacre, Bream Road, St Briavels, Glos. GL15 6TL, UK
[d] BGR, Stilleweg, 2, 30655 Hannover, Germany

Abstract

The Southern Prince Charles Mountains (SPCM) are mostly occupied by the Archaean Ruker Terrane. The Lambert Terrane crops out in the northeastern part of the SPCM. New geochemical and zircon U–Pb SHRIMP ages for felsic orthogneisses and granitoids from both terranes are presented. Orthogneisses from the Ruker and Lambert terranes differ significantly in their major and trace-element compositions. Those from the Ruker Terrane comprise two distinct groups: rare Y-depleted and abundant Y-undepleted. U–Pb isotopic data provide evidence for tonalite–trondhjemite emplacement at 3392±9 and 3377±9 Ma, pre-tectonic granite emplacement at 3182±9 Ma, metamorphism(?) at c. 3145 Ma, and thermal events at c. 1300(?) and 626±51 Ma. The Lambert Terrane orthogneisses probably originated in a continental magmatic arc. Zircon dating shows a very different geological history: pre-tectonic granitoid emplacement at 2423±18 Ma, metamorphism at 2065±23 Ma, and syn-tectonic granitoid emplacement at 528±6 Ma, syn-tectonic pegmatite emplacement at 495±18 Ma. The Lambert Terrane can be correlated with neither the Meso- to Neoproterozoic Beaver Terrane in the Northern PCM, which differs in isotopic composition, nor with the Archaean Ruker Terrane, which differs in both granitoid chemical composition and the timing of major geological events. It represents a Palaeoproterozoic orogen which experienced strong tectonic re-activation in Pan-African times. The Lambert Terrane has some geochronological features in common with the Mawson Block, which comprises south Australia and some areas in East Antarctica.
© 2005 International Association for Gondwana Research. Published by Elsevier B.V. All rights reserved.

Keywords: Orthogneiss; SHRIMP dating; Geochemistry; Precambrian; Antarctica

1. Introduction

The Prince Charles Mountains (PCM) constitute the best exposed cross section through the East Antarctic Shield, extending for over 500 km along the drainage basin of the Lambert Glacier–Amery Ice Shelf system. Early workers, on the basis of lithology and numerous Rb–Sr ages, recognised two major tectonic provinces in the PCM, roughly corresponding to the mountain belt topography. These were an Archaean province in the Southern PCM (SPCM; the Southern Zone of Solov'ev, 1972, the Southern Province of Tingey, 1991, and the Ruker Terrane of Mikhalsky et al., 2001), and a Meso- to Neoproterozoic province in the Northern PCM (NPCM; the Northern Zone of Solov'ev, 1972, the Northern Province of Tingey, 1991, and the Beaver–Lambert Terrane of Mikhalsky et al., 2001). It should be noted that Solov'ev (1972), having no isotopic ages from this region, suggested that his Southern Zone was Palaeo- to Mesoproterozoic, whereas the Northern Zone — Archaean.

Kamenev et al. (1993) proposed a threefold subdivision of the area on structural and lithological grounds. They distinguished a relatively stable South Lambert (Ruker) Province, consisting of granite–greenstone and granite–gneiss–schist belts, in the SPCM, and a North Lambert (Beaver) Province, comprising a charnockite–granulite belt which was highly mobile until Cambrian, in the NPCM. These provinces were separated by a third province of supracrustal and granitic rocks in the central part of the PCM (including the central and northern Mawson Escarpment). This area was termed the Lambert Province (Kamenev et al., 1993) and its component

* Corresponding author. Tel.: +7 921 3000656; fax +7 812 7141470.
E-mail address: emikhalsky@mail.ru (E.V. Mikhalsky).

rocks the Lambert Complex. The Lambert Province was considered to be either a tectonic 'buffer' zone formed by interaction between the granite–greenstone and charnockite–granulite belts at mid-crustal levels, or the higher-grade equivalents of the granite–greenstone belts themselves (Kamenev et al., 1990). Recent workers (Boger et al., 2001; Fitzsimons, 2003) termed this area the Lambert Terrane, but explained its geological features differently. Boger et al. (2001) considered the Lambert Terrane a Cambrian suture and correlated it with a high-grade belt exposed in the Prydz Bay area, while Fitzsimons (2003) supported this model, but noted that c. 550–500 Ma tectonism was reported only from the Mawson Escarpment. The crustal prehistory of the Lambert Terrane was not discussed by these authors.

The Beaver and Lambert terranes were considered to be sections of an extensive Meso- to Neoproterozoic mobile belt extending through most of the peripheral part of the East Antarctic Shield (the Late Archaean–Proterozoic Wegener–Mawson Mobile Belt of Kamenev, 1991, and Circum-Antarctic Mobile belt of Yoshida, 1992, 1994). Fitzsimons (2000) considered the NPCM as a part of the Rayner Province extending from western Enderby Land to the Lambert Glacier area.

Kamenev and Krasnikov (1991) distinguished yet another tectonic province, the Fisher Terrane, in the central PCM, based on its distinctive lithology and geological history. This terrane is characterized by essentially calc-alkaline magmatism, and probably represents an active continental margin or a collage of island arcs and foreland domains (Mikhalsky et al., 1996, 1999).

The geochemical features of granites and felsic orthogneisses from the Ruker and Beaver terranes have been the subject of detailed studies by Sheraton and Black (1988) and Sheraton et al. (1996). These authors described the chemical evolution of granitic rocks in the PCM and adjacent areas, including the Archaean cratons, but concentrated on either Archaean orogenic or Early Palaeozoic post-orogenic granitoids, and did not distinguish Proterozoic orthogneisses of the northern SPCM (Lambert Terrane) as a separate unit. They considered this area as part of the Beaver Terrane, but new isotopic data (see below) preclude such a correlation.

In this paper we present new geochemical and U–Pb isotopic (SHRIMP) data for rocks from the Lambert and Ruker terranes obtained by earlier Russian Antarctic expeditions and by the Prince Charles Mountains Expedition of Germany and Australia (PCMEGA 2002/2003), and address the hitherto enigmatic relationships between these areas. The main goal of this study is to compare the age data and compositional features of the two terranes and highlight their significant differences.

2. Geological background

Most of the SPCM (the area south of about 72° 30′S) are underlain by the Ruker Terrane, except for the central and northern Mawson Escarpment, together with a few nunataks to the north and west (e.g., Mt Johns and Shaw Massif), which have not yet been studied in detail, and probably belong to the Beaver Terrane (Fig. 1). However, the age and composition of many outcrops in this area remain not sufficiently studied, so that the true extent of the Lambert Terrane is not yet clear.

The Ruker Terrane comprises an Archaean granite–gneiss basement (Mawson Orthogneiss and variously deformed granitic plutons), which appears to be overlain by a variety of metasedimentary and metavolcanic rocks of three distinct lithological units: the Menzies, Ruker, and Sodruzhestvo Series. The age of the presumed granitic basement and overlying metasediments was first determined by Rb–Sr studies, whole-rock isochron ages of 2700 ± 90, 2750 ± 400, and 2760 ± 200 Ma being reported by Tingey (1982). A few imprecise Meso- to Neoproterozoic ages were also obtained (1400 ± 150 Ma, 1170 ± 230 Ma, c. 1040 Ma, c. 830 Ma; Tingey, 1982; Mikhalsky et al., 2001, and references therein). These were interpreted as reset ages, and provide some evidence for Mesoproterozoic thermal reworking of the area, possibly in response to high-grade metamorphism in the NPCM. Muscovite-bearing pegmatites cutting the metasediments were dated at 2589, 2100, 1995, and 1708 Ma, and it was suggested that Palaeoproterozoic, as well as Archaean, sequences may be present (Tingey, 1982). Conventional zircon U–Pb studies gave an age of 3005 ± 57 Ma for the Mt Ruker granite pluton, and showed that zircon crystallization in metasedimentary and metavolcanic rocks in the same area occurred between 3200 and 2500 Ma ago, with a prominent thermal event at 532 ± 20 Ma (Mikhalsky et al., 2001). Recent zircon SHRIMP studies on rocks from the southern Mawson Escarpment (Boger et al., 2001) gave ages of c. 3370 Ma (interpreted as representing inheritance from the source region), 3160 Ma (maximum age of deformation), and 2650 Ma (pegmatite crystallization and minimum age of deformation). Sm–Nd whole-rock and mineral data for mafic metamorphic rocks of volcanic and plutonic origin from Mt Ruker define isochron ages of 2917 ± 82 and 2878 ± 65 Ma, respectively (Beliatsky et al., 2003), which probably represent the time of metamorphism, although low Nd_i values (0.50845, 0.50799) preclude long pre-metamorphic crustal residence times. Hornblende–biotite granite gneisses from the southern Mawson Escarpment have given a Sm–Nd whole-rock isochron age of 3230 ± 130 Ma; tonalitic orthogneisses from the same area have given very imprecise Sm–Nd whole-rock and mineral (orthopyroxene, plagioclase)-whole-rock isochron ages of c. 3000 and c. 1900 Ma, respectively (Mikhalsky et al., in press).

The Late Archaean Menzies Series includes pelitic and calcareous metasediments, amphibolites, and conglomerates, commonly associated with prominent thick white to greenish quartzite units. It typically contains lower amphibolite-facies assemblages of relatively high-pressure Barrovian type (staurolite+kyanite±garnet). Presumably late Archaean Ruker Series consists of relatively low-grade (greenschist facies) mafic to felsic schists (probably metavolcanic rocks) and associated metadolerite sills, metapelitic schist, slate, phyllite, diamictite (tillite?), and banded ironstone. Metamorphosed mafic and ultramafic rocks occur as boudins, lenses, and blocks within high-strain shear zones in the southern Mawson Escarpment. The presumed (?Neo) proterozoic Sodruzhestvo Series is also
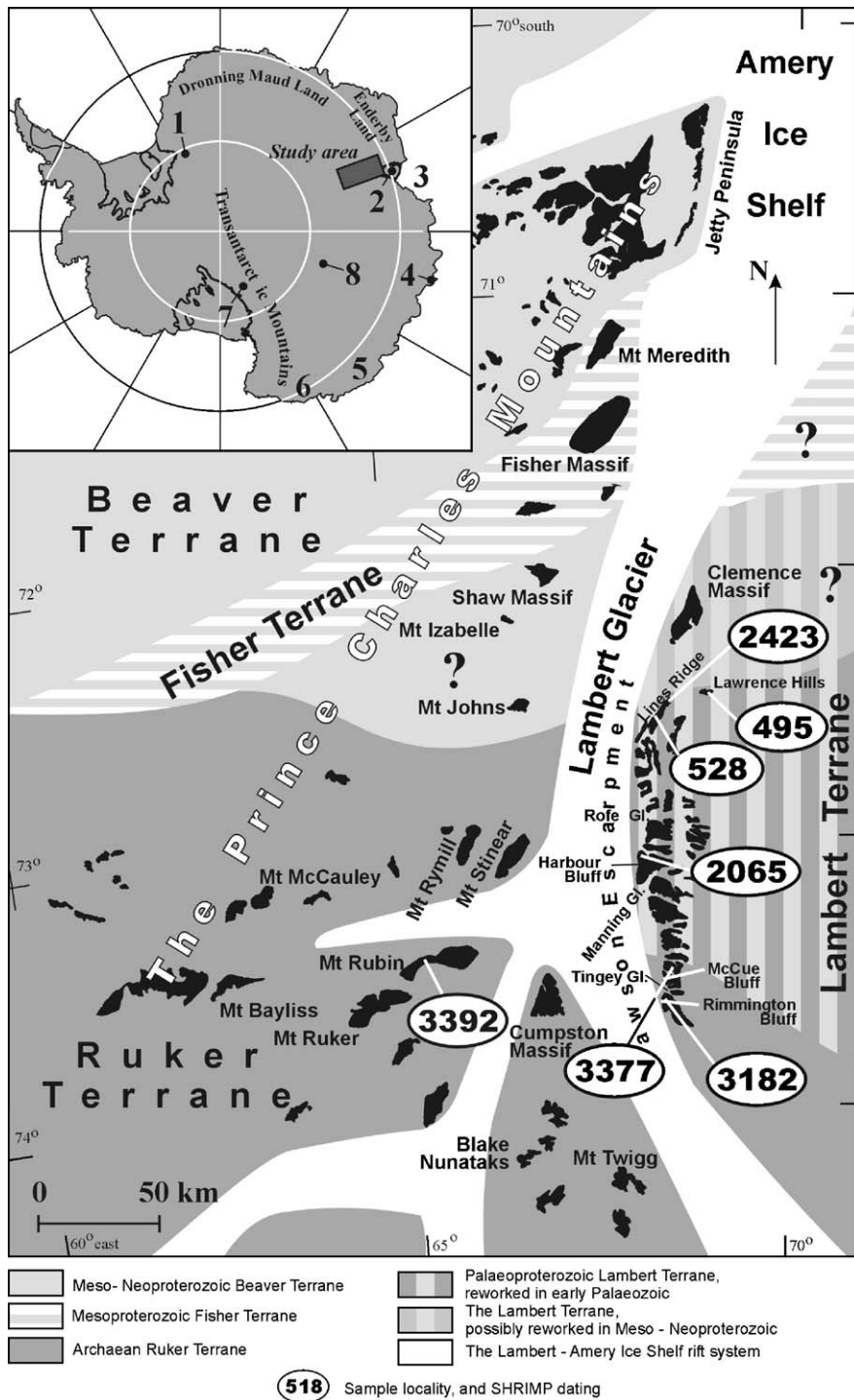
Fig. 1. The Prince Charles Mountains, showing tectonic subdivisions and the isotopic data locations. Numbers in the inset are: 1 — the Shackleton Range, 2 — the Amery Ice Shelf, 3 — Prydz Bay, 4 — Denman Glacier and Bunger Hills, 5 — Adelie Land, 6 — George V Land, 7 — Miller Range, 8 — Vostok Station and the subglacial lake.

of greenschist facies, but of more calcareous composition (metapelitic and calcareous schist, phyllite, and slate, with minor marble, quartzite, and diamictite). Its metamorphism appears to be prograde, and original sedimentary features (cross-bedding, ripple marks) are locally preserved. The granitic basement and metasedimentary cover are cut in many localities by mostly metamorphosed and commonly deformed dolerite dykes considered to be Palaeo- to Mesoproterozoic on

geochemical grounds (Sheraton and Black, 1981). The age of regional metamorphism of the Ruker Terrane is uncertain, but it was tentatively correlated with the late Mesoproterozoic to early Neoproterozoic (c. 1000 Ma) event which resulted in formation of the Beaver Terrane by Tingey (1991). However, there is evidence for a relatively high-grade (up to granulite-facies) Archaean event, and possibly other events at c. 2500 and 1900 Ma (Mikhalsky et al., 2001). Widespread retrogres-

sion, and possibly prograde metamorphism of the Sodruzhestvo Series occurred during a Pan-African or Ross age (c. 500 Ma) event in which locally abundant granitic rocks were emplaced.

The northern part of the SPCM (including most of the Mawson Escarpment) is underlain by upper amphibolite-facies (locally transitional to granulite-facies) rocks collectively named the Lambert Complex. Leucocratic biotite and garnet–biotite gneiss, granite–gneiss, and rare plagiogneiss (probably orthogneiss), as well as mesocratic garnet–biotite±hornblende plagiogneiss (probably paragneiss) and mafic amphibolite, are the most common rock types. Calc-silicate rocks and marble form relatively thick units at some localities. The rocks were intruded by abundant early Palaeozoic pegmatite and granite sheets, dykes, and vein networks (c. 500 Ma, Tingey, 1991, and references therein). Concordant amphibolite and mafic granulite layers occur in places, possibly being deformed relics of intrusive rocks, but mafic dykes are generally rare. Metagabbro and ultramafic rocks occur as tectonic slabs and blocks in the northern Mawson Escarpment (Rofe Glacier, Lawrence Hills).

The Beaver Terrane occupies the NPCM and consists mainly of high-grade (upper amphibolite to granulite-facies) metamorphic rocks formed in the late Mesoproterozoic to early Neoproterozoic (c. 1000–940 Ma; Tingey, 1982; Kinny et al., 1997; Carson et al., 2000; Boger et al., 2000). The Fisher Terrane is largely composed of much lower-grade (amphibolite facies) schist and gneiss of probable volcanic origin, intruded by a number of gabbro to granite plutons. This assemblage crops out on Fisher Massif and a few surrounding exposed areas, although its real extent is debatable. Volcanic activity was dated at c. 1300 Ma by both conventional (Beliatsky et al., 1994) and SHRIMP (Kinny et al., 1997) zircon studies. Emplacement of intrusives ceased by about 1190 Ma, lower amphibolite-facies metamorphism occurred at c. 1100 Ma, and late granitoids were emplaced at c. 1020 Ma (Mikhalsky et al., 2001, and references therein). Most of these ages do not correlate with known events in the Beaver Terrane, although similar ages (c. 1300 Ma, c. 1100 Ma) were recently obtained by SHRIMP zircon studies of granite–gneisses from Mt Meredith (A. A. Laiba, personal communication).

3. Geochemistry of basement orthogneisses

About one hundred samples of felsic metamorphic rocks and pre- to syn-tectonic granitoids from the SPCM were analysed for major and trace elements at Bundesanstalt für Geowissenschaften und Rohstoffe (BGR, Hannover) and Geoscience Australia (Canberra) by X-ray fluorescence spectrometry. Samples collected by Australian geologists in the 1970s, by Russian geologists in the 1980s, and by the PCMEGA 2002/2003 participants are included. Representative analyses are listed in Table 1.

Analysed rocks from the Ruker Terrane (RT) and the Lambert Terrane (LT) have distinct mineralogical and chemical compositions. In the RT biotite–quartz–feldspar and hornblende–biotite–feldspar gneisses of tonalite, granodiorite, and monzogranite composition (following the classification of Le Maitre, 1989) are common rock types, although much of the felsic orthogneisses are of granitic composition. Tonalitic and trondhjemitic gneisses (plagiogneisses) are common in some areas, particularly in the southern Mawson Escarpment, Cumpston Massif, Blake Nunataks, and Mt Twigg. Compositionally similar rocks form granitoid plutons elsewhere in the RT (Mounts Ruker, Rymill, Stinear, and Bayliss). These bodies are generally less strongly deformed than the felsic orthogneisses, but may grade locally into granitic gneiss. In the LT garnet–biotite–quartz–feldspar and biotite–quartz–feldspar granodiorite–syenogranitic gneisses predominate. Felsic gneisses commonly form layered units, and in some localities thin sheet-like bodies occur. Larger (up to 700 m) deformed plutons occur in some localities. Younger (Pan-African) granitic rocks occur as dykes and locally abundant veins throughout much of the LT. The composition range of these rocks will be discussed in a separate paper.

SiO_2 contents mostly range from 60% to 78% (Fig. 2) with only a few intermediate compositions, as on the northern Mawson Escarpment (Lines Ridge) and at Clemence Massif. Some garnet–biotite±hornblende plagiogneisses, as well as a number of amphibolites, have 46–57% SiO_2, but mineral and chemical compositions indicate sedimentary or mafic magmatic (cumulate) origins. These rocks are not, therefore, included into the present study.

Most rocks are marginally peraluminous to metaluminous, with alumina-saturation index (ASI, $Al_2O_3/(CaO+Na_2O+K_2O)$, mol.%) between 0.7 and 1.15, so that they can be classified as I-type (derived by melting of igneous source rocks: Chappell and White, 1974). Only a few samples have ASI>1.1.

On a normative Ab–Or–An diagram the RT and LT rocks plot in distinct fields, with only slight overlap (Fig. 3). Most RT rocks plot in the trondhjemite and granite fields of Barker (1979), whereas LT rocks are mainly granodiorite and granite, with some tonalite. This chemical classification apparently differs from the modal scheme of Le Maitre (1989) mentioned above. The LT rocks thus plot on a generally more calcic (An-rich) trend. The samples from both terranes show considerable scatter on a normative Q–Ab–Or diagram (not presented), consistent with several distinct rock suites being present, although many samples plot near the isobaric minima and therefore likely represent near-minimum melts, as there is no field association which could suggest that the granites are fractionates of more mafic compositions.

The analysed rocks form generally coherent trends of decreasing Al_2O_3, CaO, TiO_2, Fe_2O_3(total), and P_2O_5, with increasing SiO_2 (Fig. 4), although the scatter is generally large, which is partly due to the presence of geochemically distinct rock groups. The RT gneisses form two distinct groups: high-Y (>35 ppm) and low-Y (<30 ppm) (Fig. 5). The low-Y group is much less abundant and comprise rocks from the south-eastern part of the SPCM. The LT rocks also include a few high-Y samples, but those are mostly garnet-bearing and may represent sedimentary-derived melts or paragneiss.

Table 1
Chemical compositions of felsic metamorphic rocks and granitoids from the SPCM (major components — wt.%, trace elements — ppm)

Sample ID	48111-1	V29	73281071	33536	33515-3	73281557	33504	48110-1	48114-4	73281137	48104-4	48104-1	73281376	33507-1
Locality	Clemence Massif	Lines Ridge	Mount Izabelle	Harbour Bluff	Mawson Escarp.	Mawson Escarp.	Lines Ridge	Clemence Massif	Rofe Glacier	Shaw Massif	Rofe Glacier	Rofe Glacier	Mount Johns	Lines Ridge
Rock type	Bt–Cpx gneiss	Bt–Hbl granitoid	Hb–Bt gneiss	Bt augen gneiss	Bt gneiss	Bt gneiss	Bt granite gneiss	leuco-gneiss	Hbl–Bt gneiss	Bt gneiss	Bt gneiss	Bt gneiss	Bt gneiss	Bt granite gneiss (sheet)
	The Lambert Terrane													
SiO_2	57.04	57.56	65.40	65.77	66.63	68.50	69.47	69.81	70.59	71.30	71.37	73.01	73.20	74.09
TiO_2	0.9	1.11	0.61	0.78	0.74	0.57	0.53	0.26	0.22	0.40	0.42	0.25	0.38	0.10
Al_2O_3	16.59	16.76	15.72	15.28	14.75	14.70	14.52	15.02	14.90	13.78	13.36	13.70	13.29	13.90
$Fe_2O_3^*$	9.18	7.26	1.44	5.28	5.90	0.87	3.58	2.72	0.33	0.50	0.54	1.95	1.05	0.86
FeO	nd	nd	3.75	nd	nd	3.40	nd	nd	1.47	2.15	2.69	nd	1.15	nd
MnO	0.16	.10	0.10	0.04	0.06	0.04	0.03	0.06	0.02	0.05	0.03	0.02	0.04	0.01
MgO	3.62	2.68	1.55	1.23	1.43	1.10	1.23	0.74	0.54	0.56	0.98	0.70	0.54	0.20
CaO	6.73	4.76	4.45	1.75	2.73	2.71	2.41	3.00	2.47	1.78	0.79	1.05	1.40	1.16
Na_2O	3.19	4.02	3.00	3.00	3.20	3.40	3.40	4.39	3.04	3.00	1.80	2.84	3.00	2.82
K_2O	1.32	4.10	2.98	5.32	3.39	3.49	3.48	2.07	5.27	4.44	7.05	5.71	5.17	5.91
P_2O_5	0.22	.48	0.11	0.51	0.26	0.21	0.23	0.08	0.66	0.11	0.14	0.05	0.12	0.03
LOI	0.52	.43	0.36	0.23	0.14	0.58	0.15	1.36	0.82	0.58	0.68	0.32	0.20	0.25
Cr	152	52	45	58	57	18	40	53	nd	9	nd	14	7	35
Ni	44	25	8	21	21	9	21	32	nd	3	nd	7	3	13
V	128	87	62	44	67	32	41	20	nd	23	nd	15	17	10
Pb	6	27	18	46	21	20	4	11	55	29	50	55	35	47
Zn	125	108	91	52	60	54	33	48	nd	62	nd	27	46	5
Rb	68	76	96	296	117	141	88	44	125	190	273	196	166	107
Ba	463	1584	959	992	839	642	1168	749	nd	820	nd	461	906	2074
Sr	371	629	334	168	166	193	488	480	255	210	88	85	211	327
Ga	21	24	17	16	20	17	17	17	nd	18	nd	17	18	16
Nb	8	14	6	17	17	14	16	3	3	10	19	15	12	2
Zr	87	507	171	376	269	253	214	146	6	240	145	191	240	37
Y	12	40	26	67	21	14	25	bdl	13	26	13	12	22	7
Th	bdl	14	6.0	59.0	25.0	38	50.0	bdl	5.5	45.0	24.8	54.0	24.0	16.0
U	8	4	1.0	8.0	3.0	1.5	3.0	bdl	bdl	2.5	7.1	13.0	1.5	3.0
La	25	157	22	126	40	49	73	35	nd	14	nd	65	73	44
Ce	41	256	49	234	81	91	146	43	nd	148	nd	109	131	49

Sample ID	33013-8	73281541	73281048A	72280758	48136-1	33129-6	73281238	48154-8	48151-7	73281918	73281917	73281297	48168-6	73281723
Locality	Mawson Escarp.	Mount Bayliss	Mount McCauley	Mount Stinear	Mount Stinear	McCue Bluff, top	Cumpston Massif	Mawson Escarp.	Cumpston Massif	Mount Twigg	Mount Twigg	Blake Nunataks	Mount Rubin	Mount Ruker
Rock type	Hbl–Bt gneiss	Bt granite gneiss	Hbl–Bt granite gneiss	Bt–Hbl granite gneiss	Bt gneiss	Bt plagio-gneiss	Hbl–Bt granite gneiss	Hbl granite gneiss	Hbl–Bt granite gneiss	Bt gneiss	Bt gneiss	Ms–Bt gneiss	Bt tonalite (cobble)	Bt granite
	The Ruker Terrane, Y-undepleted group					The Ruker Terrane, Y-depleted group							Granitoids	
SiO_2	68.52	69.70	71.00	71.10	74.08	68.54	68.50	58.84	68.81	72.00	73.70	75.50	70.21	72.00
TiO_2	0.68	0.68	0.78	0.82	0.39	0.42	0.30	0.87	0.33	0.17	0.22	0.05	0.38	0.16
Al_2O_3	12.15	13.33	12.34	12.22	12.33	15.88	15.93	15.37	16.01	15.16	14.61	14.57	15.82	14.16
$Fe_2O_3^*$	8.04	1.31	1.41	1.06	3.00	3.25	0.97	7.33	2.95	0.20	0.31	bdl	1.17	0.46
FeO	nd	3.00	3.70	3.60	nd	nd	1.75	nd	nd	1.30	1.15	0.50	1.15	1.35
MnO	0.12	0.07	0.07	0.07	0.07	0.05	0.04	0.12	0.05	0.01	0.03	bdl	0.03	0.05
MgO	0.20	1.07	0.72	0.58	0.18	1.19	0.71	4.28	0.65	0.30	0.44	0.09	1.09	0.23
CaO	2.99	2.43	2.29	2.52	1.14	2.94	3.17	6.89	3.30	1.22	1.43	2.23	1.33	0.96
Na_2O	3.74	3.35	2.40	3.10	3.63	5.36	5.85	3.63	5.14	3.95	4.20	5.10	6.06	3.45
K_2O	2.63	3.93	4.62	4.12	4.50	1.38	1.39	1.53	1.82	5.23	3.98	1.39	1.30	5.47
P_2O_5	0.18	0.23	0.22	0.22	0.08	0.13	0.09	0.23	0.08	0.06	0.09	0.03	0.22	0.06
LOI	0.36	0.76	0.46	0.62	0.18	0.40	0.46	0.49	0.42	0.46	0.18	0.28	1.63	0.58
Cr	80	27	12	10	11	78	bdl	107	11	7	11	bdl	nd	3
Ni	3	19	6	7	4	16	3	69	8	3	5	7	nd	3
V	5	50	27	28	bdl	41	20	157	22	9	12	3	nd	7
Pb	4	27	27	13	28	4	4	bdl	7	58	20	27	22	32
Zn	206	68	71	53	60	66	42	91	38	25	28	6	nd	26
Rb	45	188	220	151	146	46	28	61	39	196	118	54	55	256

Table 1 (*continued*)

Sample ID	33013-8	73281541	73281048A	72280758	48136-1	33129-6	73281238	48154-8	48151-7	73281918	73281917	73281297	48168-6	73281723
Locality	Mawson Escarp.	Mount Bayliss	Mount McCauley	Mount Stinear	Mount Stinear	McCue Bluff, top	Cumpston Massif	Mawson Escarp.	Cumpston Massif	Mount Twigg	Mount Twigg	Blake Nunataks	Mount Rubin	Mount Ruker
Rock type	Hbl–Bt gneiss	Bt granite gneiss	Hbl–Bt granite gneiss	Bt–Hbl granite gneiss	Bt gneiss	Bt plagio-gneiss	Hbl–Bt granite gneiss	Hbl granite gneiss	Hbl–Bt granite gneiss	Bt gneiss	Bt gneiss	Ms–Bt gneiss	Bt tonalite (cobble)	Bt granite
	The Ruker Terrane, Y-undepleted group						The Ruker Terrane, Y-depleted group						Granitoids	
Ba	1751	696	720	705	862	150	547	220	944	739	415	523	nd	595
Sr	237	256	68	84	62	339	835	297	818	200	278	246	100	118
Ga	20	18	16	16	21	23	20	18	22	19	17	17	nd	19
Nb	23	29	61	60	48	8	4	8	6	7	11	5	7	17
Zr	742	378	535	570	636	188	131	174	130	91	159	68	196	197
Y	49	69	89	85	80	12	9	26	bdl	7	18	3	17	25
Th	5.0	18.0	35.0	25.0	18.0	5.0	4.0	bdl	bdl	49.0	16.0	13.0	9.7	43.0
U	3.0	4.0	5.0	2.0	4.0	3.0	1.0	3.0	bdl	6.5	0.5	4.0	bdl	4.0
La	38	62	112	112	96	29	10	bdl	24	32	37	3	48	75
Ce	78	134	213	192	163	52	25	31	49	64	70	47	104	137

bdl — below determination level; nd — no data. FeO — by wet chemistry when determined.

There are some systematic differences between orthogneiss samples from the two terranes. Most RT rocks (high-Y group) have, for a given SiO_2 content, lower Al_2O_3, and possibly total alkalis, whereas Fe_2O_3, TiO_2 and P_2O_5 tend to be higher. Fewer trace-element data are available, but the RT rocks tend to be more depleted in the large-ion lithophile elements (LILE) Rb, Pb, Ba, and Th and relatively enriched in the high-field strength elements (HFSE) Zr, Nb, and Y. Average concentrations of trace elements in the RT high-Y felsic gneisses are (in ppm; $n=24$) Rb 132, Pb 18, Ba 672, Th 19, Zr 455, Nb 32, Y 70. The LT rocks have average concentrations (in ppm; $n=33$) Rb 150, Pb 31, Ba 863, Th 26, Zr 233, Nb 12, Y 26. It is noteworthy that the RT low-Y group has similar trace-element compositions to the LT rocks in terms of the HFSE (Zr, Nb, Y, Ti, P), but not in terms of the LILE Rb, Pb, Ba (in ppm; $n=9$): Rb 77, Pb 19, Ba 597,

Th 13, Zr 195, Nb 9, Y 20. Contents of other trace elements (Sr, U, Ga, Zn) are within similar ranges. Most RT rocks have Ga/Al in the range 2.2–3.2 (average 2.78), whereas LT rocks are between 2.0 and 2.8 (average 2.39). There are also systematic differences in Ce/Y ratios (and, by analogy, REE). The RT high-Y rocks have $Ce_N/Y_N=2.8-6.3$ and low-Y $Ce_N/Y_N=3.0-25.0$. The LT rocks mostly have moderately to strongly fractionated Ce_N/Y_N (4.8–18.0). They are thus comparable in this respect to the RT low-Y group, with which they share quite similar major-element compositions (Figs. 4 and 5), although there are significant differences in trace-element compositions. The RT and LT rocks have similar K/Rb (150–520 and 150–450) and Rb/Sr (0.1–6.3 and 0.2–3.1, respectively).

On primitive mantle-normalized spiderdiagrams (Fig. 6) most RT rocks (the high-Y group) show moderate LILE enrichment, small to moderate negative Nb anomalies, large Sr and Ti anomalies, and pronounced positive Zr anomalies. In contrast, LT rocks are generally more strongly enriched in
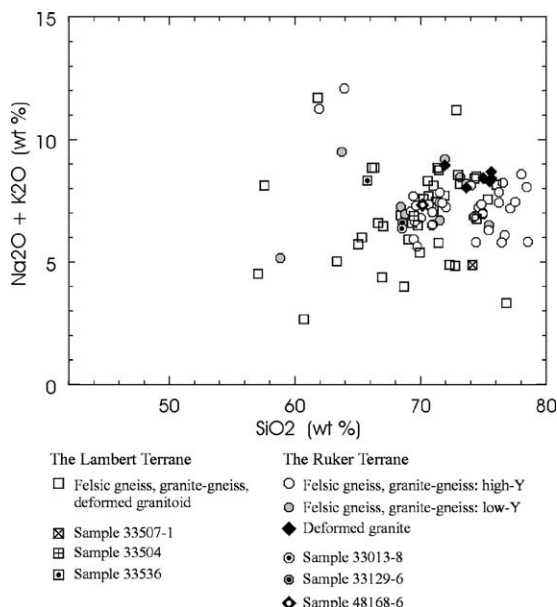

Fig. 2. SiO_2 vs total alkali plot for metamorphic rocks and granitoids from the Ruker and Lambert terranes.
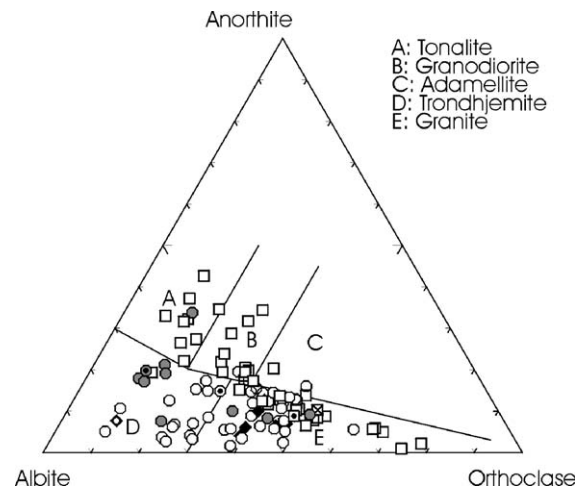

Fig. 3. Normative albite–orthoclase–anorthite plot. Fields after Barker (1979). Symbols as in Fig. 2.
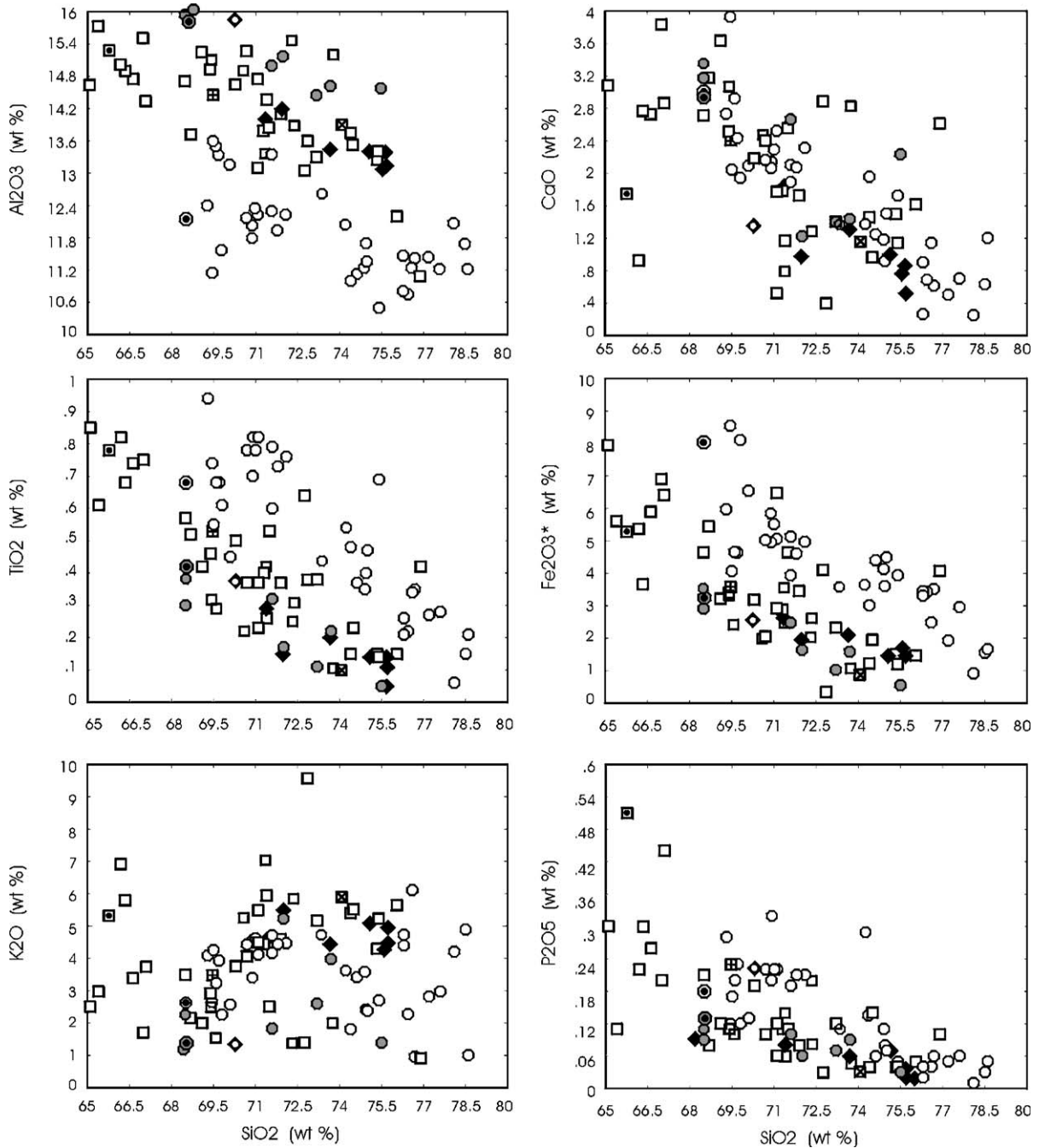
Fig. 4. SiO$_2$ vs major oxide plots. Symbols as in Fig. 2.

LILE, and have larger Nb anomalies, but smaller Sr, Zr, and Ti anomalies, producing a less fractionated (less spiky) pattern. Compared to both these groups, the low-Y RT rocks have low HFSE (Nb, P, Zr, and Ti) and LREE, but much higher Sr (small positive or negative anomalies). These rocks have distinctive (mainly trondhjemitic) compositions, and crop out in scattered localities in the southern Mawson Escarpment, Cumpston Massif, Blake Nunataks, and Mt. Twigg, that is in the south-eastern part of the RT. The high-Y RT rocks crop throughout the RT, including the south-eastern part. A Pan-African granitic sample 33507-1 from the LT has marked Nb, P, Zr, Ti, and Y depletion.

4. Geochronology

Seven samples were selected for zircon U–Pb isotopic analysis. The measurements were carried out with a SHRIMP-II ion microprobe at the Centre for Isotopic Research (VSEGEI, St. Petersburg, Russia). Zircon grains were hand selected and mounted in epoxy resin, together with chips of the TEMORA (Middledale Gabbroic Diorite, New South Wales, Australia) and 91500 (Geostandart zircon) reference zircons. The grains were sectioned approximately in half and polished. Five to ten zircon grains from each sample were studied. Each analysis consisted of 5 scans through the mass range; the spot
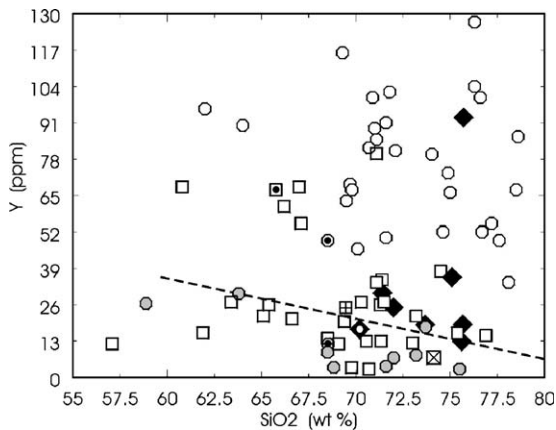
Fig. 5. SiO$_2$ vs Y plot. Dashed line divides the Y-depleted and Y-undepleted orthogneiss groups of Sheraton and Black (1981). Symbols as in Fig. 2.

diameter was about 18 ìm and the primary beam intensity about 4 nA. The data were reduced in a manner similar to that described by Williams (1998, and references therein), using the SQUID Excel Macro of Ludwig (2000). The Pb/U ratios were normalised relative to a value of 0.0668 for the ^{206}Pb/^{238}U ratio of the TEMORA zircon, equivalent to an age of 416.75 Ma (Black and Kamo, 2003). Uncertainties given for individual analyses (ratios and ages) are at the one σ level, whereas uncertainties in calculated concordia ages are reported at the two σ level.

Samples 48168-6, 33129-6, and 33013-8 were collected from the RT, and samples 33504, 33536, 33507-1, and 48113-6 came from the LT. The data are presented in Table 2.

4.1. Ruker Terrane

Sample 48168-6 is a granitic cobble from a Sodruzhestvo Series diamictite (probably a tillite) at Mt Rubin. It is a coarse-grained biotite-bearing porphyritic tonalite with little or no secondary alteration. It has low HFSE contents, and apparently is similar to the low-Y group orthogneisses.

Zircon grains are prismatic ($l>2.0$, $l=$grain length/width ratio) with no terminal faces. A few grains are long-prismatic. Smaller grains are metamict, except in thin outer zones. Distinct rims are rare. Zircons are not transparent, many grains containing abundant inclusions which produce a very dark (nearly black) color. Most grains have a reddish tint, probably due to hematite inclusions. Cathodoluminescent (CL) images highlight grain inhomogeneity, with irregular darker and lighter areas (Fig. 7A). The darker areas tend to form outer zones and have low Th/U ratios (0.06–0.23), whereas lighter areas have higher Th/U (0.46–0.57). Th and U contents vary widely, with higher U in the outer areas.

Eight analyses on five zircon grains were obtained. Six analyses from low-U inner zones are nearly concordant on a U–Pb isotopic ratio plot (Fig. 8A), and give a weighted mean ^{207}Pb/^{206}Pb age of 3392±6 Ma. Two high-U rim analyses are discordant, producing ^{206}Pb/^{238}U ages of 2085 and 735 Ma. The latter analysis plots rather close to the lower intercept with the concordia. All eight analyses lie along a discordia line with

an upper intercept at 3395±9 Ma and a lower intercept at 626±51 Ma (MSWD=0.40). The date of c. 3395 Ma is interpreted to be the tonalite crystallization age, and the age of c. 600 Ma probably represents a thermal overprint.

Sample 33129-6 was collected from the upper surface of McCue Bluff in the southern Mawson Escarpment. It is a grey fine-grained banded gneiss containing up to 5 vol.% of green biotite and subordinate hornblende. Mineral phases do not show any alteration. The rock is of trondhjemitic composition and belongs to the Y-depleted group. Zircon grains vary in size and shape (Fig. 7B). Larger (>0.1 mm) grains are cloudy or transparent, light pinkish, and prismatic to slightly rounded. Short-prismatic ($l=1.7$–2.5) grains predominate. Inner thin oscillatory zoning is prominent and cores are distinguishable in some larger grains.

Eleven analyses on nine zircon grains were obtained. All analyses, except one apparent rim (5.1) are homogeneous in
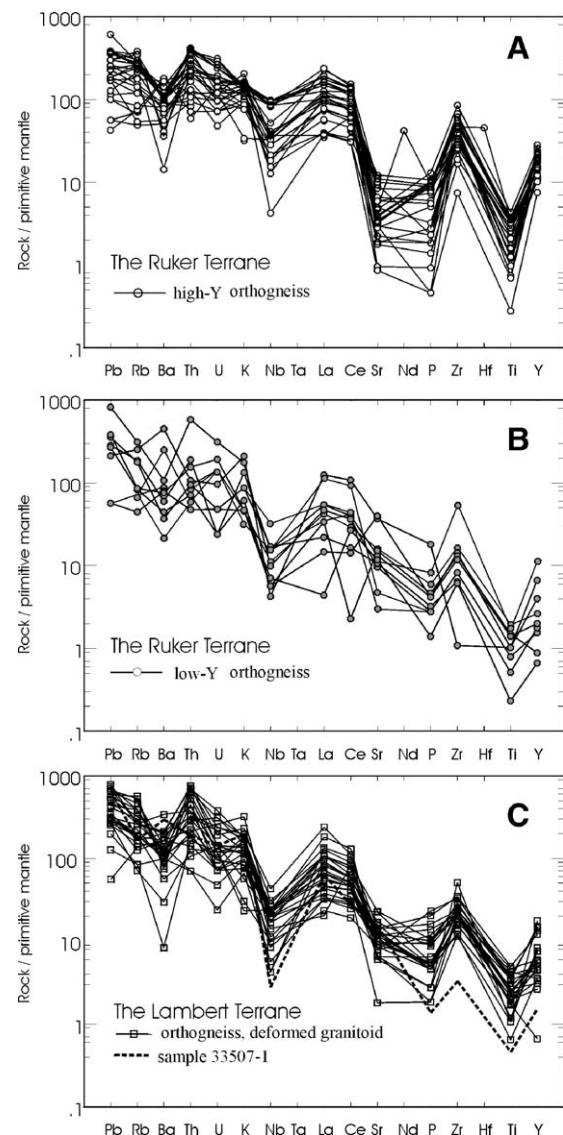

Fig. 6. Primitive mantle normalized spiderdiagrams for orthogneisses from the Ruker Terrane (A, B) and Lambert Terrane (C). Normalization factors from Sun and McDonough (1989).

Table 2
U–Pb isotopic compositions of zircons from the SPCM

Grain spot	U (ppm)	Th (ppm)	^{232}Th/^{238}U	^{206}Pb* (ppm)	Ages (Ma)		Radiogenic ratios						Errcorr
					^{206}Pb/^{238}U	^{207}Pb/^{206}Pb	^{207}Pb*/^{206}Pb*	±%	^{207}Pb*/^{235}U	±%	^{206}Pb*/^{238}U	±%	
Sample 48168-6													
1.1	939	539	0.59	571	3447±180	3388.1±3.7	0.28455	0.24	27.7	6.7	0.707	6.7	0.999
2.1	318	74	0.24	200	3533±180	3401.3±8.8	0.28700	0.57	28.9	6.7	0.73	6.7	0.996
3.1	217	99	0.47	140	3609±190	3412.7±6.6	0.28910	0.42	29.9	6.7	0.75	6.7	0.998
3.2	489	93	0.20	312	3577±180	3406±4.6	0.28784	0.29	29.4	6.7	0.742	6.7	0.999
4.1	467	230	0.51	290	3491±180	3393.1±5.1	0.28547	0.33	28.3	6.7	0.719	6.7	0.999
5.1	1160	187	0.17	447	2382±130	3259.8±4.3	0.26216	0.27	16.2	6.7	0.447	6.7	0.999
5.2	420	209	0.52	244	3295±170	3361.8±7.2	0.27980	0.46	25.7	6.7	0.667	6.7	0.998
5.3	3111	201	0.07	359	774±49	1756±40	0.10740	2.2	1.89	7	0.1275	6.7	0.951
Sample 33129-6													
1.1	293	126	0.44	170	3334±50	3377.5±6.8	0.2826	0.44	26.39	2.0	0.677	1.9	0.976
2.1	353	152	0.45	204	3322±50	3375±6.2	0.2822	0.40	26.23	2.0	0.674	1.9	0.980
3.1	348	152	0.45	201	3307±50	3376.6±6.4	0.2825	0.41	26.10	2.0	0.670	1.9	0.978
3.2	226	99	0.45	128	3268±51	3301.8±8.1	0.2693	0.51	24.51	2.0	0.660	2.0	0.968
1.2	117	44	0.39	65.4	3238±53	3345±11	0.2768	0.71	24.90	2.2	0.652	2.1	0.947
4.1	183	103	0.58	107	3355±60	3379.3±9.8	0.2830	0.63	26.64	2.4	0.683	2.3	0.965
5.1	1635	90	0.06	881	3140±47	3145.3±4.7	0.2439	0.29	21.10	1.9	0.628	1.9	0.988
6.1	400	324	0.84	242	3436±52	3389.1±6.4	0.2847	0.41	27.64	2.0	0.704	1.9	0.979
7.1	461	183	0.41	278	3426±52	3385.8±6.2	0.2841	0.40	27.48	2.0	0.701	1.9	0.980
8.1	347	210	0.62	203	3349±52	3372.5±7.9	0.2817	0.51	26.46	2.0	0.681	2.0	0.969
9.1	257	231	0.93	150	3335±52	3365±8.3	0.2804	0.53	26.19	2.1	0.678	2.0	0.967
Sample 33013-8													
1.1	296	165	0.58	161	3159±50	3184.6±9.2	0.2500	0.58	21.80	2.1	0.632	2.0	0.961
1.2	216	103	0.49	118	3175±52	3181±10	0.2494	0.64	21.88	2.2	0.636	2.1	0.955
2.1	122	67	0.57	64.4	3078±54	3110±14	0.2386	0.85	20.13	2.3	0.612	2.2	0.932
3.1	528	275	0.54	283	3128±48	3172.4±7.1	0.2480	0.45	21.36	2.0	0.624	2.0	0.974
4.1	130	71	0.56	75.2	3325±61	3170±15	0.2476	0.96	23.05	2.5	0.675	2.3	0.925
4.2	183	79	0.44	105	3311±52	3243±16	0.2594	0.99	24.01	2.2	0.671	2.0	0.895
5.1	331	129	0.40	182	3197±49	3184.3±6.9	0.2499	0.43	22.12	2.0	0.642	1.9	0.976
6.1	493	193	0.40	269	3169±48	3179.3±5.9	0.2491	0.37	21.81	1.9	0.635	1.9	0.982
7.1	718	338	0.49	316	2669±42	3129.7±6.1	0.2415	0.39	17.07	2.0	0.513	1.9	0.981
7.2	443	184	0.43	229	3031±46	3168.2±6.4	0.2474	0.40	20.48	2.0	0.600	1.9	0.979
8.1	102	44	0.45	55.6	3177±53	3187±12	0.2504	0.73	21.99	2.2	0.637	2.1	0.944
Sample 33504													
1.1	1547	521	0.35	469	1948±25	2338.8±5.5	0.14938	0.32	7.27	1.5	0.3529	1.5	0.977
1.2	775	499	0.67	198	1675±22	2430.8±8.1	0.15766	0.48	6.45	1.6	0.2968	1.5	0.953
1.3	603	170	0.29	218	2266±29	2401.7±7.8	0.15498	0.46	9.00	1.6	0.4212	1.5	0.957
2.1	652	220	0.35	242	2318±29	2458.8±7.1	0.16030	0.42	9.56	1.6	0.4327	1.5	0.962
2.2	318	141	0.46	113	2226±29	2420±11	0.15664	0.63	8.91	1.7	0.4125	1.5	0.925
5.1	270	113	0.43	98.9	2283±29	2446±12	0.15910	0.7	9.32	1.7	0.4249	1.5	0.909
5.2	866	152	0.18	318	2290±29	2396.4±6.6	0.15451	0.39	9.09	1.5	0.4265	1.5	0.968
5.3	440	220	0.52	169	2385±30	2441.4±8.8	0.15866	0.52	9.79	1.6	0.4477	1.5	0.947
6.1	426	107	0.26	156	2294±30	2410.4±9.1	0.15579	0.53	9.18	1.7	0.4274	1.6	0.947
6.2	372	190	0.53	136	2281±29	2419.3±9.6	0.15660	0.57	9.17	1.6	0.4245	1.5	0.936
Sample 33536													
1.1	793	13	0.02	268	2140±12	2120±22	0.13160	1.3	7.15	1.4	0.3938	0.63	0.443
1.2	793	12	0.02	262	2094.2±8.8	2050.4±9.2	0.12653	0.52	6.697	0.72	0.3838	0.49	0.685
1.3	180	37	0.21	66.3	2302±100	2329±60	0.14850	3.5	8.79	6.3	0.4290	5.2	0.829
1.4	205	24	0.12	70.7	2179±60	2088±39	0.12930	2.2	7.17	3.9	0.4020	3.3	0.825
2.1	234	66	0.29	69.1	1900±24	2155±25	0.13430	1.4	6.35	2.0	0.3427	1.5	0.724
2.2	145	60	0.43	43.1	1906±32	2085±18	0.12900	10.0	6.12	2.2	0.3440	2.0	0.891
2.3	968	14	0.01	341	2214±160	2096±110	0.12980	6.1	7.34	10.0	0.4100	8.4	0.809
2.4	1186	17	0.01	439	2307.3±9.1	2051±36	0.12650	2.1	7.51	2.1	0.4303	0.47	0.222
3.1	154	63	0.43	52	2136±26	2203±17	0.13800	0.97	7.48	1.7	0.3928	1.4	0.829
3.2	353	33	0.10	116	2088±44	1993±67	0.12250	3.8	6.46	4.5	0.3825	2.5	0.549
3.3	929	15	0.02	319	2166±18	2106±39	0.13060	2.2	7.19	2.4	0.3992	0.98	0.401

Table 2 (continued)

Grain spot	U (ppm)	Th (ppm)	^{232}Th/^{238}U	^{206}Pb* (ppm)	Ages (Ma)		Radiogenic ratios						Errcorr
					^{206}Pb/^{238}U	^{207}Pb/^{206}Pb	^{207}Pb*/^{206}Pb*	±%	^{207}Pb*/^{235}U	±%	^{206}Pb*/^{238}U	±%	
Sample 33507-1													
1.2	492	53	0.11	36.1	527.6±8	434±42	0.05550	1.9	0.653	2.4	0.0853	1.6	0.645
1.3	1907	181	0.10	142	533.2±7.7	534±33	0.05811	1.5	0.691	2.1	0.0862	1.5	0.702
2.1	1618	144	0.09	120	535.6±7.7	495±21	0.05708	0.96	0.682	1.8	0.0866	1.5	0.843
2.2	2031	174	0.09	150	532.4±7.7	512±20	0.05754	0.91	0.683	1.8	0.0861	1.5	0.854
2.3	501	56	0.12	35.9	516±8.7	559±42	0.05880	1.9	0.675	2.6	0.0833	1.8	0.674
3.1	491	47	0.10	34.4	491.5±7.6	373±140	0.05400	6.1	0.590	6.3	0.0792	1.6	0.256
3.2	1840	162	0.09	137	535.1±7.7	577±19	0.05926	0.87	0.707	1.7	0.0865	1.5	0.864
4.1	1625	147	0.09	119	525.2±7.8	473±35	0.05653	1.6	0.662	2.2	0.0849	1.6	0.703
4.2	1163	134	0.12	86	532.3±7.7	518±25	0.05768	1.1	0.685	1.9	0.0861	1.5	0.799
Sample 48113-6													
1.1	2272	45	0.02	206	607±39	486±130	0.05690	5.9	0.775	9	0.0988	6.7	0.750
2.1	2425	17	0.01	171	502±32	480±44	0.05670	2	0.633	7	0.0810	6.7	0.959
3.1	4550	60	0.01	153	245±16	406±33	0.05484	1.5	0.293	6.9	0.0388	6.7	0.977
4.1	2338	11	0.00	162	497±32	521±32	0.05777	1.4	0.638	6.9	0.0801	6.7	0.978
5.1	4391	53	0.01	161	270±18	441±22	0.05571	0.98	0.329	6.8	0.0428	6.7	0.989
6.1	2085	20	0.01	145	501±32	546±26	0.05844	1.2	0.651	6.8	0.0808	6.7	0.984
7.1	2104	53	0.03	218	600±39	743±440	0.06400	21	0.860	22	0.0976	6.9	0.310
8.1	6566	64	0.01	199	224±15	316±21	0.05271	0.93	0.257	6.8	0.0353	6.7	0.991
9.1	2315	60	0.03	189	503±33	661±270	0.06160	13	0.690	14	0.0812	6.8	0.472
9.2	4440	60	0.01	186	303±20	363±51	0.05380	2.3	0.357	7.1	0.0481	6.7	0.947

Note. Common Pb corrected using measured ^{204}Pb. Errors are 1-sigma. Error in standard calibration was 2.27% (not included into above errors). Pb* indicates the radiogenic Pb portion.

terms of U and Th contents and Th/U ratio (0.4–0.9). Eight analyses are nearly concordant and yield a weighted mean ^{207}Pb/^{206}Pb age of 3376.9±8.8 Ma (Fig. 8B). Two core (or inner zone) analyses are discordant with ^{207}Pb/^{206}Pb ages of 3302 Ma (3.2), and 3345 Ma (1.2). The latter point lies along a reference line defined by the nearly concordant analyses, with a highly imprecise lower intercept age of about 1300 Ma. The last analysis (5.1) was from a relatively wide high-U rim; it is concordant and has a ^{207}Pb/^{206}Pb age of 3145 Ma. The date of 3377±9 Ma probably reflects granitoid emplacement. A thermal (metamorphic?) event occurred at c. 3145 Ma, and possibly also in the Mesoproterozoic (at c. 1300? Ma).

Sample 33013-8 was collected from the northern part of Rimmington Bluff. It is a light grey coarse-grained gneissic Y-undepleted granite with mylonitic augen structure, containing biotite and hornblende (10–15%). There is no secondary alteration. Zircon grains are greyish-pink and mostly short-prismatic ($\underline{l}$=2.5–3.0), although long-prismatic grains also occur (l=5.0, Fig. 7C). Most grains are fractured, transparent, and commonly show thin internal oscillatory zoning. Many contain small darker cores of prismatic or rounded shape. These zircons are similar to those in sample 33129-6, but the zoning is less pronounced.

Eleven analyses on eight zircon grains were obtained. All analyses have very similar U, Th, and Th/U (0.4–0.6). The inner (core) and outer zones have similar isotopic compositions and gave overlapping ages. Six analyses (four inner and two outer zones) are concordant and yield a weighted mean ^{207}Pb/^{206}Pb age of 3179.5±9.4 Ma (Fig. 8C). The other analyses plot outside the cluster, but three out

of five plot on a regression line (discordia) with an upper intercept at 3181.9±7.7 and a lower intercept at 587±170 Ma (MSWD=0.14). The discordant analyses (except 4.2) are from zircon cores. The older age could represent granitoid emplacement or a metamorphic event. However, although the inner and outer zones are indistinguishable in terms of isotopic composition, a magmatic origin is more likely as the grain shape does not provide any evidence for recrystallisation. A magmatic origin may be suggested by the relatively high Th/U ratios, and similar ratios are also typical of other RT samples which have better field evidence (rock structure) for a magmatic origin. In this sample the zircon cores may have been inherited from the source region, but their isotopic signatures were completely blurred during crystallization. This may be suggested by the wide scatter of model ^{206}Pb/^{238}U ages of the cores between 2669 and 3325 Ma.

Analysis 2.1 is nearly concordant at about 3110 Ma. However, this age may have no geological significance as the point is only slightly outside the main cluster. In contrast, the lower intercept age (c. 600 Ma) likely reflects Pan-African thermal activity.

4.2. Lambert Terrane

Sample 33504, from the northern tip of Lines Ridge, is a light pinkish-grey, slightly layered, coarse-grained, gneissic leucocratic biotite (2–3%) granodiorite. This rock was collected from a large (more than 700 m across) deformed granitic body grading into felsic gneiss. It has low Y (25 ppm) and may be referred to as Y-depleted. Most zircon grains are
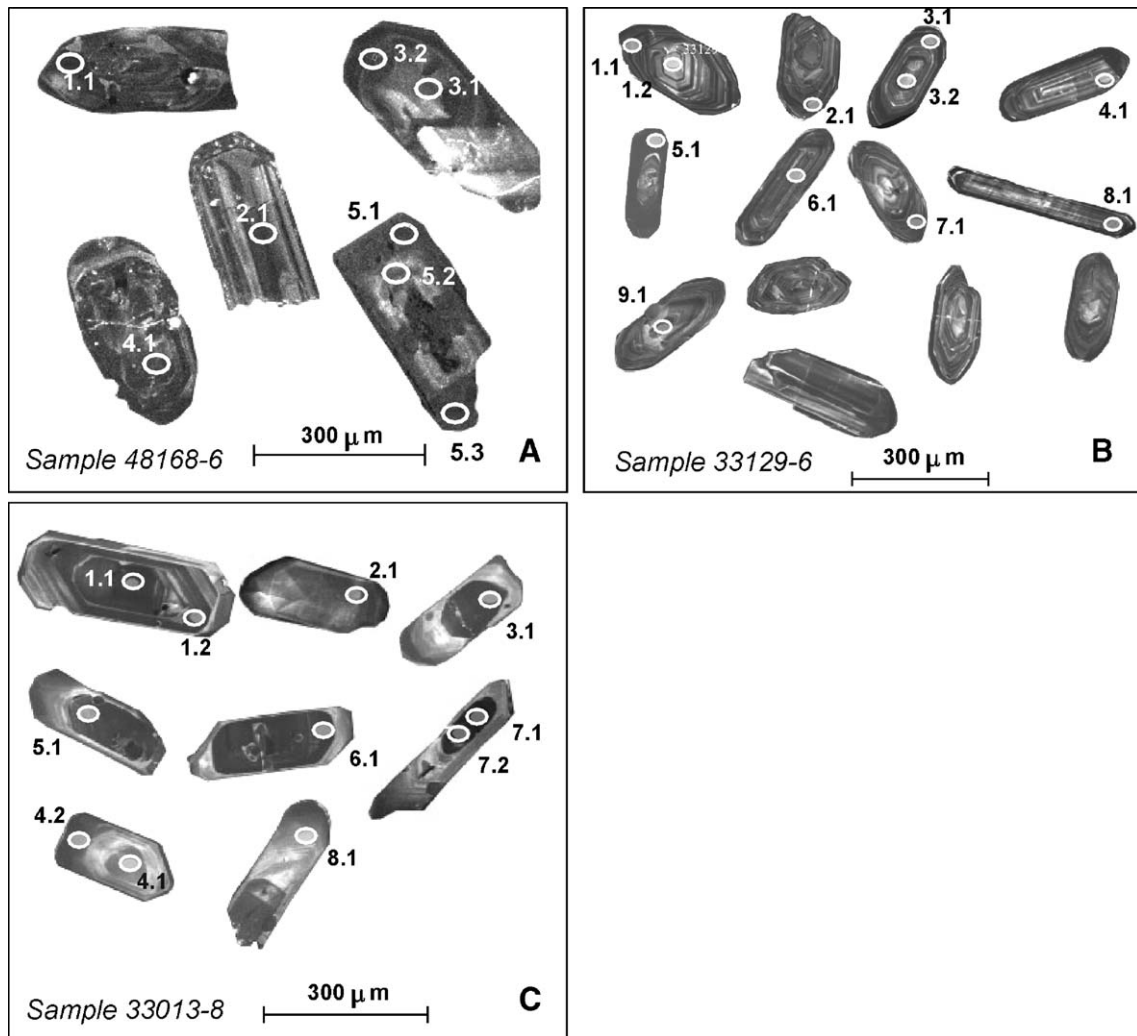
Fig. 7. Cathodoluminescent images of zircons from the Ruker Terrane samples.

non-transparent due to fracturing, and are brownish-pink; smaller grains appear more transparent. They are generally somewhat rounded, short-prismatic ($l = 1.7-2.4$), with well-developed bipyramid faces (Fig. 9A); near-isometric ($l = 1.3$) or elongated ($l = 3.3$) grains are rare. Thin oscillatory zoning tends to occur in the inner zones.

Ten analyses on four zircon grains were obtained. Most analyses are indistinguishable in terms of Th, U, and Th/U (0.18–0.64). One grain has high Th (500 ppm) in both inner (point 1.1) and outer (point 1.2) zones, the two analyses being strongly discordant. The other eight analyses (of both inner and outer zones) form a coherent, but slightly discordant, cluster (Fig. 10A) with $^{207}Pb/^{206}Pb$ ages of 2396–2459 Ma. All ten analyses define a poorly constrained reference line with an upper intercept at 2402 ± 9 Ma, and a lower intercept at -142 ± 100 Ma (MSWD = 1.4). A line forced through point $t(0 \pm 50$ Ma) gives an upper intercept at 2423 ± 18 Ma (MSWD = 0.92), interpreted as the time of granodiorite emplacement.

Sample 33536, from the northern tip of Harbour Bluff, represents a scarce relic of country rocks heavily invaded by abundant granite and pegmatite sheets and veins. It is a banded,

schistose, coarse-grained, mesocratic biotite (10–15%) augen gneiss. This rock has high Y (67 ppm) content not typical for the LT. Feldspar augen are up to 2 cm across, and make up to 20 vol.% of the rock. Biotite forms a prominent schistosity, and apatite is a conspicuous accessory. The vast majority of zircon grains recovered from this sample are pinkish-grey and fractured, but nevertheless transparent. They are relatively small (<300 μm), isometric to short-prismatic, and somewhat rounded to oval; a few grains are elongated prismatic (Fig. 9B). A distinctive feature of these zircons is the occurrence of highly luminescent (bright in CL) irregular inner zones, enclosed by lower luminescent (dark in CL) rims. A few very dark magenta spherical grains were also recovered, but these were too small to be analysed.

Eleven analyses on three zircon grains were obtained, of which six came from the light-coloured inner zones and five from the dark outer zones. The dark zones have high U (800–1200 ppm) and very low Th (12–17 ppm), resulting in very low Th/U (0.01–0.02). The light inner (core?) zones have lower U and somewhat higher Th, but Th/U is still low (0.1–0.4). The data show considerable variation in isotopic ratios, as well as in measurement precision. Most analyses are to some
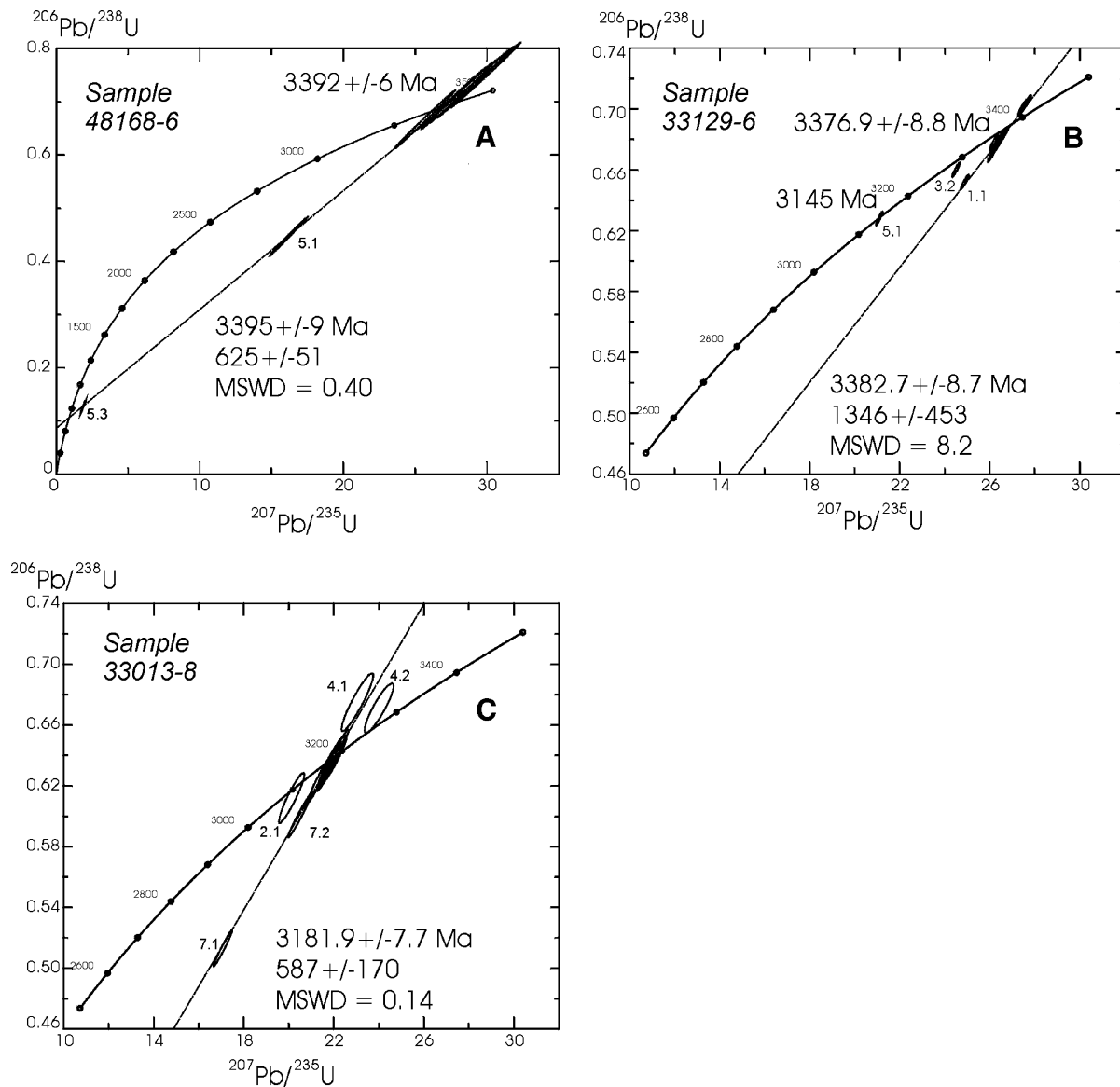
Fig. 8. U−Pb isotope diagrams for zircons from the Ruker Terrane samples.

extent discordant, and tend to be reversely discordant (Fig. 10B). Those of the outer dark zones show less scatter, but are also reversely discordant. Eight analyses give a weighted mean $^{207}Pb/^{206}Pb$ age of 2065±23 Ma. One analysis (1.3) gives a nearly concordant $^{207}Pb/^{206}Pb$ age of 2329±30 Ma. Low Th/ U ratios are typical of metamorphic zircon and the rounded isometric grain shape is also consistent with a metamorphic origin. We thus interpret the date of 2065±23 Ma as a metamorphic age, and c. 2330 Ma as reflecting inheritance, possibly from an intrusive protolith.

Sample 33507-1 was collected from the central part of Lines Ridge, about 0.5 km south of sample 33504. It represents the abundant subhorizontal granitoid sheets intruded concordantly into melanocratic plagiogneiss. In places granitoid sheets are tightly folded into mesoscopic (intrafolial) folds. The rock is a light reddish, very coarse-grained, leucocratic biotite granite. Biotite is largely replaced by chlorite, and plagioclase by saussurite. The host plagiogneiss contain 30−35% dark brown

biotite, and abundant apatite, zoisite, zircon, and monazite, suggesting a sedimentary origin. Zircon grains are cloudy to semi-transparent, greyish-pink, and of various sizes (100− 400 μm: Fig. 9C). Most grains are short-prismatic (*l*=2.0−2.3) with bipyramid faces; many are somewhat rounded, and uneven or lobate (corroded) margins are common. Complex inner structures may be seen under CL, some grains displaying bright irregular inner zones; in a few cases small cores may be distinguished.

Ten analyses on four grains were obtained. Most have high U (1000−2000 ppm) and relatively low Th/U (0.06−0.12). All except two analyses (1.1 and 3.1) form a coherent cluster of concordant or slightly discordant points (Fig. 10C), with a weighted mean $^{206}Pb/^{238}U$ age of 528±6 Ma (MSWD=0.69). Analysis 3.1 is reverse discordant. Analysis 1.1, of a small inner area, which may be a relict core, is discordant, with a model $^{207}Pb/^{206}Pb$ age of 976 Ma. A reference line drawn through all the analyses yields a poorly constrained upper intercept at
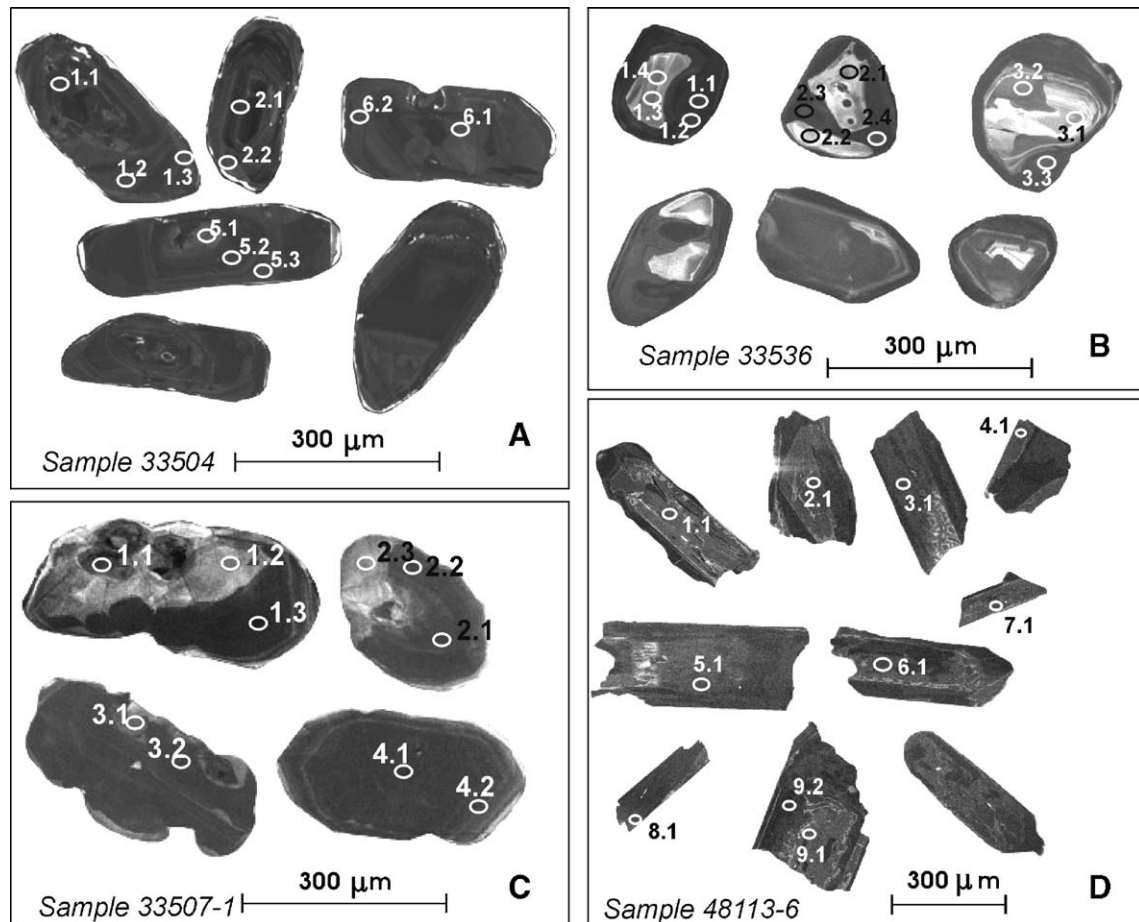
Fig. 9. Cathodoluminescent images of zircons from the Lambert Terrane samples.

1712±225 Ma. This age, although imprecise, may indicate a thermal event at the Palaeoproterozoic–Mesoproterozoic boundary. The relict core apparently contains inherited material of that age. The c. 530 Ma age may reflect crystallization (emplacement) of the granite, which apparently predated ductile deformation and folding. Thus, Pan-African tectonothermal processes in the northern Mawson Escarpment were relatively intense, and included pre- to syn-tectonic granitoid emplacement and folding.

Sample 48113-6 represents a syn-tectonic pegmatite body within an ultramafic (orthopyroxenite) tectonic slab in the Lawrence Hills. It came from a thin (0.6 m) muscovite-bearing plagioclase-rich vein bifurcating from a thick (tens of meters), apparently not sheared, concordant body of pegmatite with sheared mafic xenoliths. Zircon forms large (mostly >300 μm), well-shaped long-prismatic ($l=2.5–3.5$), brownish-pink grains. Crystals commonly form aggregates. Many grains contain areas of different response under CL: irregular darker areas, which tend to occur as outer or randomly distributed zones, and more transparent lighter areas, which tend to be inner zones (Fig. 9D). The boundaries between these zones are highly complex and uneven. This structure probably reflects disequilibrium in the magma–fluid system (an active interaction between silicate melt and fluid phase). The darker zones are not metamict, but quite strongly fractured.

Ten analyses on nine grains were obtained. All zircons are U-rich (>2000 ppm), and the darker zones contain 4400–6500 ppm. Th contents are low (11–60 ppm), so that Th/U ratios are very low (<0.03). Four out of six analyses of light zones are concordant and yield a weighted mean $^{207}Pb/^{206}Pb$ age of 495±18 Ma (Fig. 10D), which we interpret as the crystallization age. The low Th/U ratios might indicate a metamorphic origin for these grains, but they may also reflect interaction with a lithophile element (particularly U) enriched pegmatitic fluid. The other two light zone analyses are slightly discordant, with a $^{206}Pb/^{238}U$ age of c. 600 Ma. This may reflect some inheritance of older material. Four analyses of the high-U dark zones are slightly discordant, and show some variation in $^{206}Pb/^{238}U$ age in the range 300–220 Ma. A reference line through the whole dataset gives an upper intercept at 555±48 Ma and a lower intercept at 142±28 (MSWD=1.05). The lower intercept, controlled by the dark (high-U) zone analyses, may merely reflect U redistribution caused by grain fracturing. However, this age corresponds with that of magmatism at Jetty Peninsula, some 200 km to the north, where emplacement of late Jurassic–early Cretaceous alkaline rocks (142±5 Ma, 150±5 Ma, phlogopite K–Ar data; Laiba et al., 1987) reflected initial rifting in the Lambert–Amery rift zone. Thus we suggest that the c. 140 Ma date may have some geological significance, being a thermal overprint, rather than just an artefact.
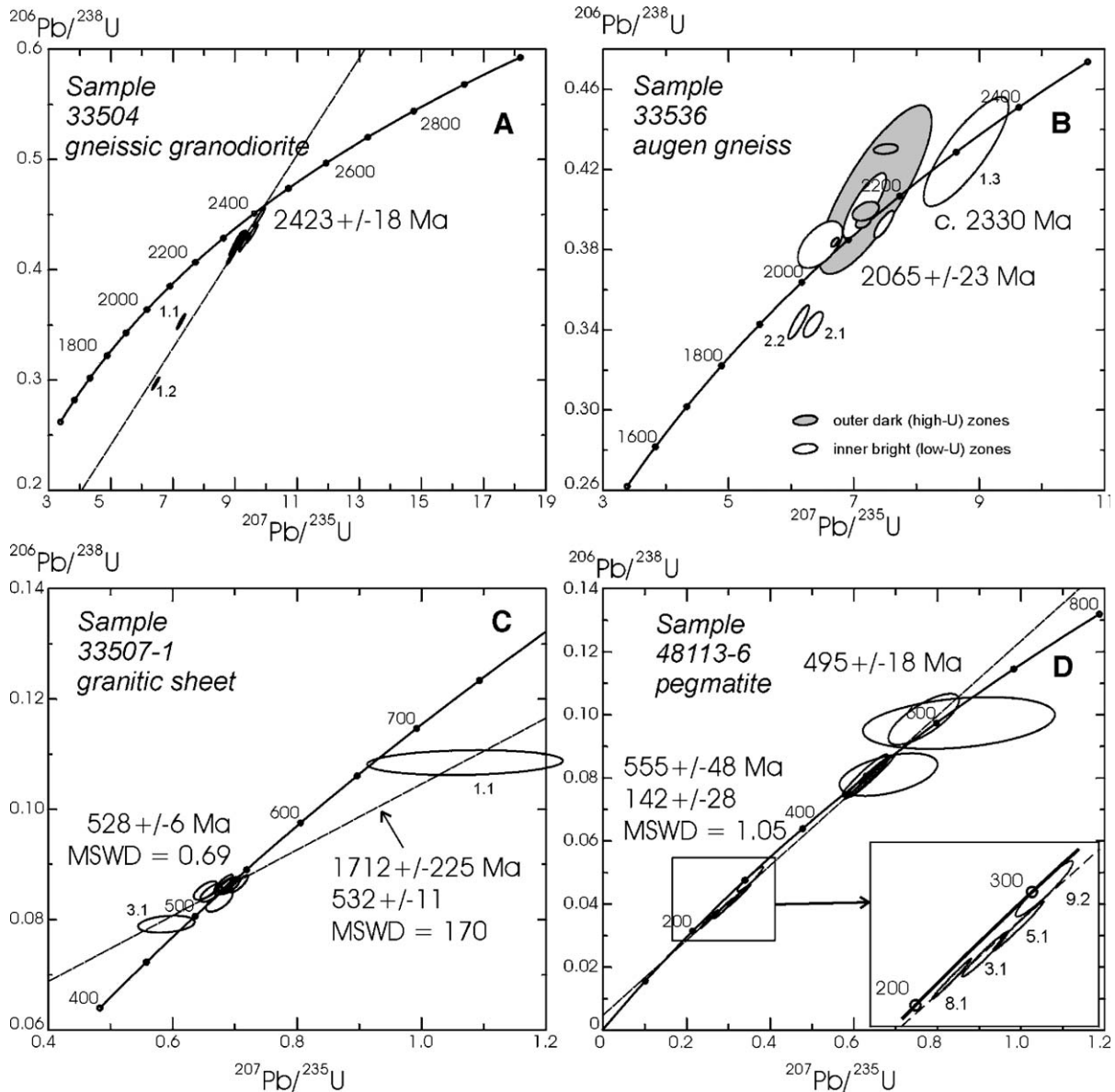
Fig. 10. U−Pb isotope diagrams for zircons from the Lambert Terrane samples.
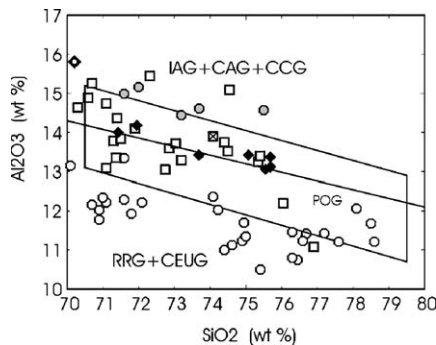

Fig. 11. A major component discrimination plot after Maniar and Piccoli (1989). RRG — rift-related granites, CEUG — epeirogenic granites, IAG — island arc granites, CAG — continental arc granites, CCG — continental collision granites, POG — postorogenic granites. Symbols as in Fig. 2.
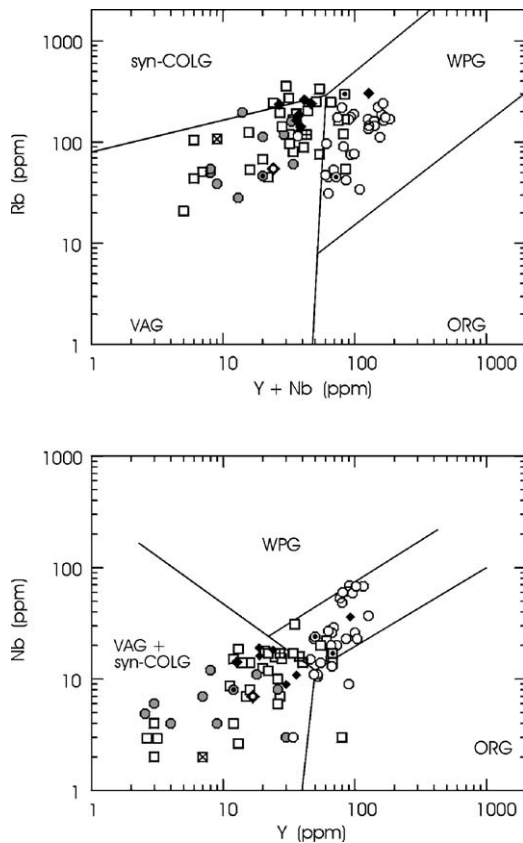
5. Discussion

Sheraton and Black (1983) first distinguished two geo-chemically distinct orthogneiss types in the Archaean of the East Antarctic Shield. These are: 1) a Y-depleted, Sr-undepleted type (mainly of tonalitic or trondhjemitic to granodioritic composition), derived by hydrous partial melting of a garnet-bearing (mafic) source and apparently representing new felsic continental crust, and 2) a Y-undepleted, Sr-depleted type (of trondhjemitic to granitic composition), formed by relatively dry melting of predominantly felsic crustal rocks. Sheraton and Black (1988) and Sheraton et al. (1996) reported that orthogneisses in the SPCM are predominantly of Y-undepleted, Sr-depleted type, and that many have chemical characteristics of A-type granites (Collins et al., 1982). The two groups plot in distinct fields on a SiO_2−Y plot (Fig. 5). The low-Y rocks in the RT are thus thought to have been derived by

Fig. 12. Trace-element discrimination plots after Pearce et al. (1984). WPG — within-plate granites, syn-COLG — syn-collisional granites, VAG — volcanic arc granites, ORG — ocean ridge granites. Symbols as in Fig. 2.

partial melting of a plagioclase-poor, garnet-bearing mafic source, and to represent mantle-derived additions to the crust. The high-Y group is enriched in other HFSE (particularly Zr and Nb), and may have been derived either by melting of an intracrustal source or, as for rocks with A-type compositions, by fractionation of Nb-rich mantle melts. However, mantle sources of these rocks would be not consistent with their isotopic features (high Sr_i, low ε_{Nd}, Tingey, 1982, Mikhalsky et al., 2001, and in press). Anyway, such compositional features are difficult to explain by simple remelting of low-Y tonalitic to granodioritic rocks in the lower crust.

The LT rocks straddle the boundary between the two types of Sheraton and Black (1983), some belonging to the Y-depleted type and others having higher Y contents, but generally not so high as those of the RT. Hence, some of these rocks may have been derived from a similar plagioclase-poor garnet-bearing mafic source region, whereas others were probably produced by remelting of older felsic crustal rocks or mixed sources.

Thus, our data generally confirm the notion of Sheraton and Black (1983) that most RT orthogneisses (high-Y) were formed by remelting of older crustal rocks, but the southeastern part also includes juvenile felsic crust derived from mafic sources. The LT rocks differ from those of the RT in terms of Y content (and other compositional features), implying a much wider involvement of mafic material in the source region(s), and

generally precluding direct remelting of the Y-undepleted RT-type source rocks.

On many discrimination diagrams the LT and RT rocks plot in different, although sometimes partly overlapping fields. On that of Maniar and Piccoli (1989) the LT rocks are generally similar to island arc–continental arc–continental collision granites, as are the RT low-Y rocks. The RT high-Y rocks tend to plot in the intraplate (rift-related and epeirogenetic) granite field and only a few within the post-orogenic field (Fig. 11). On the trace-element discrimination diagrams of Pearce et al. (1984) most LT and RT low-Y rocks plot in the volcanic-arc granite field, whereas RT high-Y rocks plot in the within-plate granite field (Fig. 12). On the discrimination diagram of Whalen et al. (1987) most LT rocks plot in or near the orogenic granite field; they are somewhat more enriched in HFSE, but not to the same extent as A-type granites (Fig. 13). The RT low-Y rocks and deformed granites are comparable to orogenic granites, whereas many high-Y rocks have distinctive A-type compositional features (high HFSE, Ga/Al>2.5, Whalen et al., 1987).

Hence, the chemical compositions of the LT granitic rocks show calc-alkaline affinities, and they probably originated in broadly orogenic, rather than anorogenic, environments. However, an origin in a immature island-arc setting is unlikely due to the relative lack of intermediate compositions, with the possible exception of the northern part of the studied area (the northern tip of the Mawson Escarpment and Clemence Massif) where some intermediate (andesitic) samples, representative of relatively thick metamorphic piles, were collected. The LT rocks differ from both the RT Y-depleted orthogneisses, which have compositions similar to typical Archaean TTG suites, and the high-Y granitoids, many of which have A-type affinities.

The age of initial extraction of continental crust from the mantle may be estimated from Sm–Nd model ages (T_{DM2}) of granitic (s.l.) orthogneisses. Typical model ages are 3.9–3.2 Ga for the RT and 3.4–3.0 Ga for the LT (Mikhalsky et al., in press). Initial ε_{Nd} values of the RT rocks are mostly between +0.5 and −5.0 at $t=3$ Ga, and of the LT rocks mostly between +2 and −1.4 (at 3 Ga), although a few values are as
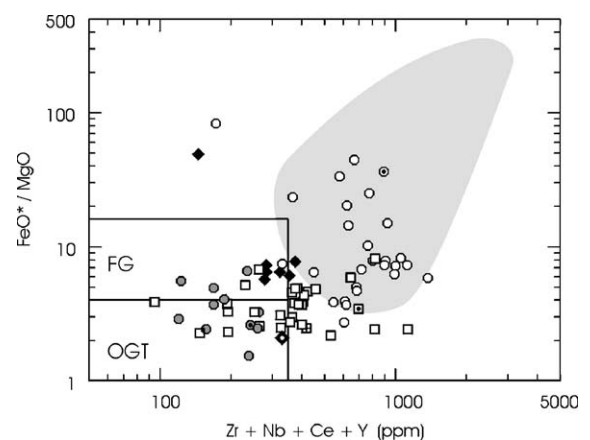

Fig. 13. Trace-element discrimination plot after Whalen et al. (1987). OGT — orogenic granite types, FG — fractionated granites, shaded field — A-type granites. Symbols as in Fig. 2.

low as −9.7. At 2.4 Ga the initial ε_{Nd} of the LT rocks would be between +6.3 and −6.4. Thus, both the RT and LT of the SPCM consist of rocks with a very long crustal history, starting in the Mesoarchaean, assuming the source regions were of depleted mantle composition. However, this may not be the case for the LT rocks, and the geochemical data discussed above suggest derivation from mafic sources which might have had lower initial ε_{Nd} as compared to the depleted mantle.

The LT rocks model ages are significantly older than those reported for the Beaver and Fisher terranes (2.3−1.4 Ga: Mikhalsky et al., 2001, in press). The Sm−Nd data provide evidence that the LT has a much longer crustal history than, and hence may not correlate with, the Beaver Terrane. This might support earlier ideas (Tingey, 1982, Kamenev et al., 1993) that the LT represents reworked Archaean assemblages, rather than juvenile Proterozoic crust. However, the geochemical differences between the two terranes, which suggest a much greater involvement of mafic sources (perhaps with lower initial ε_{Nd}) in the petrogenesis of the LT rocks, preclude a direct correlation between the RT and the LT.

Zircon U−Pb ages show that the RT and the LT experienced different tectonothermal histories. Emplacement of tonalite occurred in the RT at c. 3400 Ma, of trondhjemite, probably derived by melting of mafic rocks, at c. 3380 Ma, and of granite at c. 3180−3170 Ma (Boger et al., 2001, and this study). The minimum age of subsequent deformation is constrained by an age of c. 2645 Ma for an undeformed pegmatite (Boger et al., 2001), and might be approximated by a Sm−Nd isochron age of c. 3000 Ma (Mikhalsky et al., in press); thermal events are recorded by SHRIMP zircon ages of 3145 and 3110 Ma. Biotite granite emplacement at Mt Ruker was dated at 3005±57 Ma (conventional zircon studies, Mikhalsky et al., 2001). This granite is geochemically similar to granites at Mt Rymill and Mt Stinear, and is of near-minimum-melt composition. These granites have quite strongly fractionated REE patterns with negative Eu anomalies (Mikhalsky et al., 2001), consistent with melting of felsic crustal rocks involving plagioclase fractionation. The c. 3000 Ma granite plutons are more fractionated than most felsic orthogneisses from the RT, and their geochemistry suggests they were derived by partial melting of such rocks (Mikhalsky et al., 2001). Zircons from Ruker Series metasedimentary rocks have a wide range of isotopic ratios indicating a number of thermal events between approximately 3175 and 2500 Ma, with major Pb loss at c. 500 Ma (Mikhalsky et al., 2001). A poorly constrained Sm−Nd mineral separate (including ortho-pyroxene)-whole-rock age of c. 1900 Ma (Mikhalsky et al., in press) may reflect some Palaeoproterozoic geologic activity, although its nature remains uncertain. The very imprecise lower intercept age of c. 1300 Ma from this study could reflect yet another thermal event which was roughly co-eval with metamorphism in the Fisher and Beaver terranes to the north.

Evidence for many zircon growth events (2400, 2150, 2060, 1800, and 1600 Ma: Boger et al., 2001; this study) shows that the LT experienced a long and complex Palaeoproterozoic tectonic history. Granodiorite emplacement (at c. 2420 Ma) and high-grade metamorphism (not yet precisely dated, but the date

of c. 2065 Ma from this study may be a possible candidate) indicate an orogenic nature for at least some of these events. Thus we propose that the LT is a Palaeoproterozoic orogen, although much more work needs to be done to establish its origin and geological history. However, melting of mainly Archaean felsic crust, probably also including significant involvement of younger mafic material, during the Palaeoproterozoic is implied. Possible tectonic settings include a magmatic arc at a continental margin or a highly mature volcanic arc. Although granitic plutonism may occur during the later stages of an orogenic cycle, i.e., may be late-orogenic (Kuznetsov, 1964), the long time interval between initial continental crust formation in the Mesoarchaean (assuming derivation from a DM source) and tectonomagmatic activity in the Palaeoproterozoic suggests that the latter essentially involved crustal re-activation, rather than crust formation. In other words, the Palaeoproterozoic orogeny was likely to have been of ensialic, rather than ensimatic, nature. Nevertheless, it is possible that some Proterozoic mantle-derived material is present in the LT. For example, the mafic−ultramafic bodies in the Rofe Glacier area and Lawrence Hills, although as yet undated, may be examples of mantle derivatives or oceanic crust. Moreover, the area of exposed bedrock in the LT is quite small, and may not be lithologically representative, so that the presence of significant amounts of mafic and intermediate meta-igneous rocks cannot be ruled out. The presence of intermediate (in terms of SiO_2 content) rocks at Clemence Massif suggests a compositional peculiarity for this part of the area. A c. 800 Ma Rb−Sr age (Sr_i=0.710) reported by Tingey (1982) from Clemence Massif may indicate that this area was subject to Grenville-age metamorphism and deformation typical of the Beaver Terrane.

It is noteworthy that the spectacular (?Meso)proterozoic mafic dyke swarm in the southern Mawson Escarpment apparently terminates at the boundary between the RT and LT, defined by abrupt lithological and structural changes (Kamenev et al., 1990, Boger et al., 2001). The dyke swarm may have a northward continuation in the Manning Glacier area, where undated north−south trending metamorphosed mafic dykes are abundant.

Palaeoproterozoic tectonic activity is not well documented in Antarctica, except within the c. 1.7 Ga Mawson Block (Fanning et al., 1995). This landmass is thought to comprise the Gawler Craton (South Australia), George V Land, Adelie Land, Miller Range in the central Transantarctic Mountains, and possibly the Shackleton Range (c.f., Fitzsimons, 2003). Its geological history includes various events dated at c. 3150−2950, 2700−2350, 2000, and 1850−1700 Ma (Fitzsimons, 2003, and references therein). These ages are broadly similar to those obtained for the LT, suggesting that this part of the SPCM can be correlated with the Mawson Block. However, the RT rocks do not seem to correlate closely with the Mawson Block, being about 200 Ma older (which may be due to insufficient sampling) and having older Sm−Nd model ages. Fitzsimons (2003) concluded that one or more Mesoproterozoic sutures may lie between the Mawson Block and areas west of ~100° E (Bunger Hills), thus separating Antarctica into

at least two major tectonic domains. Nevertheless, because the RT and LT are bounded to the north by the Mesoproterozoic Fisher Terrane, which may partly correlate with the Fraser Complex of the Albany–Fraser Orogen, their correlation with the Mawson Block may be a reasonable suggestion. It should be noted, that a single zircon grain recovered from an ice drill core at Vostok Station yielded a U–Pb (SHRIMP) age of c. 1740 Ma (Leitchenkov et al., 2005). Delmonte et al. (2004) also reported Palaeoproterozoic Sm–Nd model age of bedrock fragments from the same drill core layer. These findings led additional credit to a suggestion of much wider distribution of Palaeoproterozoic events in East Antarctica than previously expected.

On the other hand, there is a large sub-glacial gap between the PCM and the Mawson Block, so that any correlation can only be speculative. Alternatively, it is worth noting that similar ages of 2550–2450, 2000–1960, 1830–1780, and 1670–1620 Ma (Cawood and Tyler, 2004) were reported from the Capricorn Orogen of Western Australia. This correlation seems very tentative as this area is separated from the SPCM not only by the Archaean and Proterozoic provinces of Australia and Antarctica, but also by the Neoproterozoic–Early Palaeozoic Darling and Prydz Bay orogens. However, in a recently proposed reconstruction, Board et al. (2005) distinguished a single Pan-African Prydz–Denman–Darling Orogen, which puts the Capricorn Orogen and the Lambert Terrane on the sides of this extensive structure. These areas remain separated by large distances anyway, but a sinistral displacement along this orogen during the Pan-African times would be consistent with well documented tectonics in Dronning Maud Land and conjugated parts of southern Africa (c.f., Jacobs and Thomas, 2004, and references therein).

At the present stage of the study it is impossible to decide whether the LT originated as a distinct Archaean complex accreted onto the adjacent RT, which then experienced Palaeoproterozoic re-activation, or whether it represents a Palaeoproterozoic section of a long-lived Meso- to Neoproterozoic polycyclic mobile belt (Kamenev et al., 1990), serving as a hinterland for the Palaeo- to Mesoproterozoic Beaver and Fisher terranes. Direct remelting of RT rocks during the genesis of the LT is unlikely. The protolith (T_{DM2}) ages of both are Archaean, but the source regions were apparently not identical.

A striking feature of the SPCM is the widespread emplacement of Pan-African granite bodies, as well as prominent deformation of similar age which caused folding and brought ultramafic material to the upper crust. Pan-African processes are widely regarded as the consequence of continental collision (e.g., Boger et al., 2001, Fitzsimons, 2003), but we believe that mafic underplating may have been an important tectonic factor as well. It should be noted that Pan-African activity was much more extensive in the LT, and was apparently confined to thermal reworking in the RT. Thus, Pan-African activity might have been largely restricted to a zone near a Proterozoic crustal-scale discontinuity (suture?) running roughly alongside the present Lambert Glacier, and defined by the distribution of Archaean (in the east side of

Lambert Glacier) and Proterozoic (in the western side of Lambert Glacier) Sm–Nd model ages (Mikhalsky et al., in press).

The LT may have been bordered by a regional transcurrent shear zone which separated older crust (Lambert and Ruker terranes) from younger crust (Beaver and Fisher terranes), which accreted southwards at a very low angle (causing no subduction-related rock associations) to the present Mawson Escarpment, thus leaving it generally unaffected during Meso- to Neoproterozoic events, with the possible exception of a thermal overprint at c. 900–800 Ma reflected by Rb–Sr ages in the northern Mawson Escarpment (Tingey, 1982). Such a discontinuity may then have been re-activated in Mesozoic times during formation of the Lambert–Amery rift system.

6. Conclusions

1. The Ruker Terrane granitic (s.l.) orthogneisses mostly originated by remelting of felsic crustal sources, although some Y-depleted rocks, which probably represent juvenile additions to the continental crust, occur in the southeastern part of the region.
2. The known geological history of the Ruker Terrane started with emplacement of tonalite–trondhjemite, derived by melting of mafic rocks, at c. 3400 and c. 3380 Ma, followed by emplacement of granite at c. 3180–3170 Ma, and thermal (metamorphic?) events at c. 3145 Ma, possibly in Mesoproterozoic time (at c. 1300? Ma), and at c. 600 Ma.
3. The geological history of the Lambert Terrane includes tectonothermal events at c. 2400 Ma (granitoid emplacement), 2065 Ma (metamorphism), and 500–550 Ma (syntectonic granitoid emplacement). A geological event may also have occurred at c. 1700 Ma.
4. Pan-African (c. 600–500 Ma) activity in the Ruker Terrane was mostly reflected by Pb loss in zircons, whereas in the Lambert Terrane mafic–ultramafic bodies were emplaced, probably by thrust tectonics, and abundant granite and pegmatite stocks and veins were intruded.
5. The Lambert Terrane is a Palaeoproterozoic orogen. Its geochemical features suggest formation in a continental magmatic arc environment, largely from protoliths derived from both felsic and mafic sources. Proterozoic mantle-derived rocks may also be present as indicated by mafic and ultramafic bodies.
6. The Lambert Terrane cannot be correlated with the Meso- to Neoproterozoic Beaver Terrane, which differs in isotopic composition, and ages, nor with the Archaean Ruker Terrane, which differs in both granitoid chemical composition, and ages.
7. The SPCM may be correlated with the Mawson Block, which comprises south Australia and some parts of East Antarctica.

Acknowledgements

References

Barker, F., 1979. Trondhjemite: definition, environment and hypotheses of origin. In: Barker, F. (Ed.), Trondhjemites, Dacites and Related rocks. Elsevier, Amsterdam, pp. 1–12.

Beliatsky, B.V., Laiba, A.A., Mikhalsky, E.V., 1994. U–Pb zircon age of the metavolcanic rocks of Fisher Massif (Prince Charles Mountains, East Antarctica). Antarctic Science 6, 355–358.

Beliatsky, B.V., Kamenev, E.N., Laiba, A.A., Mikhalsky, E.V., 2003. Sm–Nd ages of metamorphosed volcanic and plutonic rocks from Mount Ruker, the southern Prince Charles Mountains, East Antarctica. Ninth International Symposium on Antarctic Earth Sciences, Potsdam, pp. 24–25. Abstract Volume.

Black, L.P., Kamo, S.L., 2003. TEMORA 1: a new zircon standard for U–Pb geochronology. Chemical Geology 200, 155–170.

Board, W.S., Frimmel, H.E., Armstrong, R.A., 2005. Pan-African tectonism in the Western Maud Belt: P–T–t path for high-grade gneisses in the H.U. Sverdrupfjella, East Antarctica. Journal of Petrology 46, 671–699.

Boger, S.D., Carson, C.J., Wilson, C.J.L., Fanning, C.M., 2000. Neoproterozoic deformation in the Radok Lake region of the NPCM: evidence for a single protracted orogenic event. Precambrian Research 104, 1–24.

Boger, S.D., Wilson, C.J.L., Fanning, C.M., 2001. Early Paleozoic tectonism within the East Antarctic craton: the final suture between east and west Gondwana? Geology 29, 463–466.

Carson, C.J., Boger, S.D., Fanning, C.M., Wilson, C.J.L., Thost, D., 2000. SHRIMP U–Pb geochronology from Mt Kirkby, northern Prince Charles Mountains, East Antarctica. Antarctic Science 12, 429–442.

Cawood, P.A., Tyler, I.M., 2004. Assembling and reactivating the Proterozoic Capricorn Orogen: lithotectonic elements, orogenies, and significance. Precambrian Research 128, 201–218.

Chappell, B.W., White, A.J.R., 1974. Two contrasting granite types. Pacific Geology 8, 173–174.

Collins, W.J., Beams, S.D., White, A.J.R., Chappell, B.W., 1982. Nature and origin of A-type granites with particular reference to southeastern Australia. Contributions to Mineralogy and Petrology 80, 189–200.

Delmonte, B., Petit, J.R., Basile-Doelsch, I., Lipenkov, V., Maggi, V., 2004. First characterization and dating of East Antarctic bedrock inclusions from subglacial Lake Vostok accreted ice. Environmental Chemistry 1, 90–94.

Fanning, C.M., Daly, S.J., Bennett, V.C., Menot, R.P., Peucat, J.J., Oliver, R.L., Monnier, O., 1995. The 'Mawson Block': once contiguous Archean to Proterozoic crust in the East Antarctic shield and Gawler craton, Australia. ISAES VII Abstracts Volume. Siena, p. 124.

Fitzsimons, I.C.W., 2000. A review of tectonic events in the East Antarctic Shield, and their implications for Gondwana and earlier supercontinents. Journal of African Earth Sciences 31, 3–23.

Fitzsimons, I.C.W., 2003. Proterozoic basement provinces of southern and southwestern Australia, and their correlation with Antarctica. In: Yoshida, M., et al., (Eds.), Proterozoic East Gondwana: supercontinent assembly and breakup, Geological Society of London Special Publication, vol. 206, pp. 93–130.

Jacobs, J., Thomas, R.J., 2004. Himalayan-type indenter-escape tectonics model for the southern part of the late Neoproterozoic–early Paleozoic East African–Antarctic orogen. Geology 32, 721–724.

Kamenev, E.N., 1991. Structure and evolution of Precambrian cratons and metamorphic belts in East Antarctica. Sixth International Symposium on Antarctic Earth Sciences, Tokyo, pp. 261–263. Abstract volume.

Kamenev, E.N., Krasnikov, N.N., 1991. The granite(greenstone terrains in the southern Prince Charles Mountains). Sixth International Symposium on Antarctic Earth Sciences, Tokyo, pp. 264–268. Abstract volume.

Kamenev, E.N., Kameneva, G.I., Mikhalsky, E.V., Andronikov, A.V., 1990. The Prince Charles Mountains and Mawson Escarpment (in Russian). In: Ivanov, V.L., Kamenev, E.N. (Eds.), The Geology and Mineral Resources of Antarctica (in Russian). Nedra, Moscow, pp. 67–113.

Kamenev, E.N., Andronikov, A.V., Mikhalsky, E.V., Krasnikov, N.N., Stüwe, K., 1993. Soviet geological maps of the Prince Charles Mountains. Australian Journal of Earth Sciences 40, 501–517.

Kinny, P.D., Black, L.P., Sheraton, J.W., 1997. Zircon U–Pb ages and geochemistry of igneous and metamorphic rocks in the northern Prince Charles Mountains. AGSO Journal of Australian Geology and Geophysics 16, 637–654.

Kuznetsov, Iu.A., 1964. Main Types Of Magmatic Formations (in Russian). Nedra, Moscow.

Laiba, A.A., Andronikov, A.V., Egorov, L.S., Fedorov, L.V., 1987. Stock-like bodies and dykes of alkaline ultramafic rocks in Jetty Peninsula (Prince Charles Mountains, East Antarctica) (in Russian). Geologo-Geophiziches-kie Issledovanyia V Antarctike. Sevmorgeologia, pp. 35–46.

Leitchenkov, G.L., Belyatsky, B.V., Popkov, A.M., Popov, S.V., 2005. Geological nature of subglacial Lake Vostok, East Antarctica (in Russian). Data of Glaciological Studies 98, 81–91.

Le Maitre, R.W., 1989. A Classification of Igneous Rocks and Glossary of Terms. Blackwell Scientific Publications, Oxford.

Ludwig, K.R., 2000, SQUID 1.00, A User's Manual; Berkeley Geochronology Center Special Publication. No.2.

Maniar, P.D., Piccoli, P.M., 1989. Tectonic discrimination of granitoids. Geological Society of America Bulletin 101, 635–664.

Mikhalsky, E.V., Sheraton, J.W., Laiba, A.A., Beliatsky, B.V., 1996. Geochemistry and origin of Mesoproterozoic metavolcanic rocks from Fisher Massif. Antarctic Science 8, 85–104.

Mikhalsky, E.V., Laiba, A.A., Beliatsky, B.V., Stüwe, K., 1999. Geological structure of Mount Willing (Prince Charles Mountains, East Antarctica), and some implications for metamorphic rock age and origin. Antarctic Science 11, 338–352.

Mikhalsky, E.V., Sheraton, J.W., Laiba, A.A., et al., 2001. Geology of the Prince Charles Mountains, Antarctica. AGSO Bulletin, , p. 247.

Mikhalsky, E.V., Laiba, A.A., Beliatsky, B.V., in press. Tectonic subdivisions of the Prince Charles Mountains: a review of geologic and isotopic data. In: Fütterer, D.K. et al. (Eds.), Antarctica — Contributions to Global Earth Sciences. Springer, Berlin Heidelberg, New York.

Pearce, J.A., Harris, H.B.W., Tindle, A.G., 1984. Trace element discrimination diagrams for the tectonic interpretation of granitic rocks. Journal of Petrology 25, 956–983.

Sheraton, J.W., Black, L.P., 1981. Geochemistry and geochronology of Proterozoic tholeiite dykes of East Antarctica: evidence for mantle metasomatism. Contributions to Mineralogy and Petrology 78, 305–317.

Sheraton, J.W., Black, L.P., 1983. Geochemistry of Precambrian gneisses: relevance for the evolution of the East Antarctic Shield. Lithos 16, 273–296.

Sheraton, J.W., Black, L.P., 1988. Chemical evolution of granitic rocks in the East Antarctic Shield, with particular reference to post-orogenic granites. Lithos 21, 37–52.

Sheraton, J.W., Tindle, A.G., Tingey, R.J., 1996. Geochemistry, origin, and tectonic setting of granitic rocks of the Prince Charles Mountains, Antarctica. AGSO Journal of Australian Geology and Geophysics 16, 345–370.

Solov'ev, D.S., 1972. Geological structure of the mountain fringe of the Lambert Glacier and the Amery Ice Shelf. In: Adie, R.J. (Ed.), Antarctic Geology and Geophysics. Universitetsforlaget, Oslo, pp. 573–577.

Sun, S.-S., McDonough, W.F., 1989. Chemical and isotopic systematics of oceanic basalts: implications for mantle composition and processes. In: Saunders, A.D., Norry, M.J. (Eds.), Magmatism in the Ocean Basins, Geological Society of London Special Publication, vol. 42, pp. 313–345.

Tingey, R.J., 1982. The geologic evolution of the Prince Charles Mountains — an Antarctic Archean cratonic block. In: Craddock, C. (Ed.), Antarctic Geoscience. University of Wisconsin Press, Madison, pp. 455–464.

Tingey, R.J., 1991. The regional geology of Archaean and Proterozoic rocks in Antarctica. In: Tingey, R.J. (Ed.), The Geology of Antarctica. Clarendon Press, Oxford, pp. 1–58.

Whalen, J.B., Currie, K., Chappell, B.W., 1987. A-type granites: geochemical characteristics, discrimination and petrogenesis. Contributions to Mineralogy and Petrology 95, 407–419.

Williams, I.S., 1998. U−Th−Pb Geochronology by ion microprobe. In: McKibben, M.A., Shanks III, W.C., Ridley, W.I. (Eds.), Applications of Microanalytical Techniques to Understanding Mineralizing Processes, Reviews in Economic Geology, vol. 7, pp. 1–35.

Yoshida, M., 1992. Late Proterozoic to early Palaeozoic events in East Gondwana crustal fragments. XXIX International Geological Congress, Kyoto. Abstracts, vol. 2/3, p. 265.

Yoshida, M., 1994. Tectonothermal history and tectonics of Lutzow−Holm Bay area, East Antarctica: a reinterpretation. Journal of the Geological Society of Sri Lanka 5, 81–93.